1-1-2013

Using Heavy Flavors To Study New Physics

Kristopher Jason Healey
Wayne State University,

USING HEAVY FLAVORS TO STUDY NEW PHYSICS

by

KRISTOPHER J. HEALEY

DISSERTATION

Submitted to the Graduate School

of Wayne State University,

Detroit, Michigan

in partial fulfillment of the requirements

for the degree of

DOCTOR OF PHILOSOPHY

2013

MAJOR: PHYSICS

Approved by:

_____

Advisor Date

_____

_____

_____

_____

DEDICATION

Per il mio amore, Crystal. Without your patience and support I would never have been able to pursue such a selfish endeavor. I anticipate the remainder of my life will be gladly devoted to expressing my gratitude and appreciation.

ACKNOWLEDGMENTS

To my advisor, Dr. Alexey A. Petrov, I express my deep gratitude for guiding the path of a listless material scientist into the exciting world of phenomenology. If I leave you taking only a small measure of your ingenuity, dedication and your aggressive inquisition I will count myself lucky.

To my classmate and colleague and foremost, friend, Y. G. Aditya, I wish you well in your career and thank you for the collaborative work.

To my dissertation committee: Dr. Sean Gavin, Dr. Giovanni Bonvicini and Dr. Po Hu, I am extremely thankful for your willingness and desire to put my ability and knowledge to the test. I appreciate your time and effort, and I do not intend to disappoint.

I would also like to thank Dr. Robert Harr, Dr. Gil Paz, and Dr. Andrew Blechman for very helpful discussions in the development of this work.

TABLE OF CONTENTS

LIST OF TABLES

LIST OF FIGURES

CHAPTER 1

INTRODUCTION

1.1 Prologue

Our personal universe is the one we observe interact with daily; to do so without demanding a deeper comprehension of the governing mechanics only leads us to an existence causally determined by the unknown. Countless hours, years, and "lives" have been spent deepening this understanding for the benefit of all; and in the last year of my Ph.D, with the discovery of "a" Higgs-like particle, can we confidently claim that our model is complete. Or rather that it explains the majority of the physics of the Universe, sans gravity. Assuming of course we're not discussing why any of the fermions, including neutrinos, have their respective masses, or why there are exactly 3 generations of fermions; and it goes without mentioning that by "the Universe" we mean the 4.9% of the universe that is constituted by visible matter. The remainder is built from what we believe to be 26.8% Dark Matter(DM) and 68.3% Dark Energy[1, 2], and we have only hints at what the former could be comprised of. Dark Energy has a gravitationally repulsive effect and this fraction is enough to explain both the observed cosmological expansion[1, 2] and the flatness of our universe. Further detail regarding Dark Energy is beyond the scope of this thesis.

Due to not interacting with electromagnetism, dark matter is by nature difficult to detect. We have a drive in the field to model DM candidates and to calculate their experimental signatures. As their observability is expected to be small, we use decays and processes where DM participates that are otherwise suppressed in the standard model. Due to this suppression it becomes imperative that the calculation of the process, as well as all experimental background contributions, are as accurate as possible. The objectives of the calculations that follow in this thesis attempt to demonstrate these separate ideas: a DM-influenced de-

cay and its constraints; a background contribution to a suppressed SM decay, and possible intermediate contributions to a SM decay.

1.1.1 The Standard Model

The Standard Model(SM) of particle physics [3, 4, 5] is our current relativistic quantum field theory used to describe the electroweak and strong interactions. It is comprised of two groups of particles; the half-integer spin quarks (u, d, s, c, b, t), (e, μ, τ) leptons and the lepton neutrinos$(\nu_e, \nu_\mu, \nu_\tau)$) and the fundamental spin-1 gauge bosons that mediate their interactions ($W^\pm, Z^0$, bosons, the photon γ and the gluon g). All known matter is formed by bound states of these particles and the forces produced by their various interactions.

The electromagnetic interaction is mediated by the photon, and is a representation of a $U(1)$ gauge symmetry. The electroweak interaction is composed of an additional $SU(2)$ symmetry coupled to electromagnetism, and is mediated by the three W_i bosons. The strong interaction is mediated by the gluon. It has eight "color" charges and is represented by an $SU(3)$ symmetry.

The quarks and leptons are each split into 3 generations with the same quantum numbers but varied masses as seen in Table 1.1.1.

For each given symmetry Noether's Theorem dictates that there should be an associated conserved current, with a respective generator of the symmetry group. The conservation of a current of a $U(1)$ gauge symmetry gives rise to the electromagnetic charge for example, and the photon. When the symmetry is broken, non-zero masses for the gauge bosons arise (as we see very massive W and Z bosons as seen in Table 1.1.2. The Englert-Brout-Higgs-Guralnik-Hagen-Kibble [6, 7, 8] mechanism is a way to have spontaneous breaking of the electroweak $SU(2) \times U(1)$ gauge symmetry. This causes the original $U(1)$ gauge boson and three W_i $SU(2)$ bosons to mix into the photon and the massive electroweak $W^\pm$ and Z^0 bosons. A byproduct of this is of course the recently discovered spin-0 particle, the Higgs

Particle	Symbol	Mass (MeV)	Charge (e)
up quark	u	$2.3^{+0.7}_{-0.5}$	$2/3$
down quark	d	$4.8^{+0.7}_{-0.3}$	$-1/3$
electron	e	0.510999	-1
electron neutrino	ν_e	≈ 0	0
charm quark	c	$1,275 \pm 25$	$2/3$
strange quark	s	95 ± 5	$-1/3$
muon	μ	105.658371	-1
muon neutrino	ν_μ	< 0.17	0
top quark	t	$(175.5 \pm 0.6 \pm 0.8) \times 10^3$	$2/3$
bottom quark	b	4180 ± 30	$-1/3$
tau lepton	τ	$(1,776.82 \pm 0.16)$	-1
tau neutrino	ν_τ	< 15.5	0

Table 1.1.1: Standard Model Fermionic Catalog

boson. This mechanism can also give masses to the quarks and leptons through Yukawa couplings though does not give the dominant contribution to baryon(proton and neutron) masses.

Boson	Symbol	Mass (GeV)	Charge
photon	A^μ	0	0
gluon	g	0	0
Z Boson	Z^0	91.188	0
W Boson	$W^\pm$	80.385	± 1
Higgs Boson	H	≈ 125	0

Table 1.1.2: Standard Model Bosonic Catalog

1.1.2 Quantum Chromodynamics

Quantum Chromodynamics(QCD) is the quantum field theory describing the strong interaction of quarks. There is a $SU(3)$ color symmetry and the mediating gauge boson is the

gluon, g, meaning color-charged fields are invariant under transformations

$$q \to e^{i\tau^i} q, \tag{1.1}$$

where τ^i are the generators of the symmetry. The quarks are the only fermions that participate in the strong interaction.

The Lagrangian is

$$\mathcal{L}_{QCD} = i\bar{q}_f \gamma^\mu \mathcal{D}_\mu q_f - \frac{1}{4} G^a_{\mu\nu} G^{a\mu\nu}, \tag{1.2}$$

where "f" denotes the flavor of quark "q" and repeated indices are summed over. The covariant derivative is defined as

$$\mathcal{D}_\mu = \partial_\mu - \frac{i}{2} g_s \lambda^i G^i_\mu, \tag{1.3}$$

where the λ^i are the eight generators of $SU(3)$, and G are the gluon fields. QCD is an unbroken symmetry in the standard model, and thus the gauge bosons (gluons) are massless.

We define the coupling $\alpha_s = \frac{g_s^2}{4\pi}$. To obtain the matrix element for a transition we can treat the coupling constant as a small parameter and can expand our theory perturbatively. This is referred to as Perturbative QCD (pQCD). Each perturbative contribution can be described by Feynman Diagrams, a set of topological diagrams constructed using the Feynman rules derived from the Lagrangian, which contain the parameters for the vertices and legs.

The loop momenta are not observable, and are internally integrated over all momenta. This leads to a divergence. The process by which we remove these divergences is called Renormalization [9] where the divergences are canceled by redefining masses and coupling constants to include both the "bare" parts from the original Lagrangian, as well as the divergent pieces. This introduces a dependence of the coupling constant on the renormalization

scale which is defined as the scale at which higher-order terms are absorbed,

$$Q^2 \frac{\partial \alpha\left(Q^2\right)}{\partial Q^2} \quad = \quad \beta\left(\alpha\right). \tag{1.4}$$

The β function is a property of the theory and is a power series in α with $\beta_{LO} = -\beta_0 \alpha$, where β_0 depends on the number of particles involved in the loops at a given scale. Solving this equation gives the Q^2 dependence of our theory,

$$\alpha\left(Q^2\right) \quad = \quad \frac{\alpha(\mu^)}{1 + \beta_0 \alpha(\mu^2) \log Q^2/\mu^2}. \tag{1.5}$$

For QCD the value of β_0 is

$$\beta_0^{QCD} \quad = \quad \frac{11 C_A - 2 n_f}{12\pi}, \tag{1.6}$$

where $C_A = 3$ is from the $SU(3)$ gluon virtual corrections, and n_f is the number of active fermion flavors with mass less than Q^2. In the standard model with maximally 6 interaction flavors this yields $\beta_0 > \frac{7}{4\pi}$. The most recent average of the coupling constant evaluated at the weak scale is

$$\alpha_s(m_Z) \quad = \quad 0.1184(7). \tag{1.7}$$

This also lets us calculate

$$\alpha_s(m_D) \quad = \quad 0.3039. \tag{1.8}$$

It can be shown then that the positive nature of this term leads (1.5) to vanish at higher energies, making quarks unaffected by QCD. This is knows as asymptotic freedom [10]. In the limit that $Q^2 \to 0$ we see that the coupling constant goes to infinity. The most important

aspect of this is that below ≈ 1 GeV, the coupling constant is no longer a good expansion parameter. This is the energy where *confinement* allows hadrons, bound states of QCD partons, and we must turn to other phenomological methods to calculate our amplitudes.

Thus quarks and gluons are confined, in that they are not seen as free particles in nature. Only "color-neutral" hadronic bound states, mesons and baryons, are the particles that can be observed. While QCD can be calculated perturbatively in high energy regimes (greater than $\approx \mathcal{O}(1 \text{ GeV})$), low energy theory contains both perturbative and non-perturbative effects which are difficult to calculate. One method of simplifying calculations is to look for natural factorization scales that can split our theory into multiple energy regions. The heavy quarks that create bound states (charm and bottom), provide a natural scale to calculate the perturbative effects and to factor out "hard" physics and "soft" physics. When calculating low-energy physics and long-distance effects we now must also become concerned with electroweak contributions.

1.1.3 Important Decays for NP Searches

Electroweak decays of bound-state particles are of particular interest in the search for NP due to the rarity of some of the decay channels. It is logical to assume NP occurs at or below the probability of these SM-suppressed decays. This alone is not enough to be interesting; if the decay channel is unobservable experimentally then there is not much point to pursue the calculation. Luckily some experimentally-clean decay processes such as heavy meson decays to leptonic final states, are also SM-suppressed. This is where the focus of this work will be; using these experimentally available, SM suppressed decays to constrain contributions from DM and other NP.

The first is the leptonic decay of the charged $B^{\pm}(5280)$ meson, where we have noted the mass in MeV in parenthesis. The upper limits of the electron and muonic channels, and the

observed Branching Ratio(BR) of the tau weak channel are

$$\mathcal{B}r(B^{\pm} \to e^{\pm}\bar{\nu}_e) < 9.8 \times 10^{-7}, \quad (1.9)$$

$$\mathcal{B}r(B^{\pm} \to \mu^{\pm}\bar{\nu}_\mu) < 1.0 \times 10^{-6}, \quad (1.10)$$

$$\mathcal{B}r(B^{\pm} \to \tau^{\pm}\bar{\nu}_\tau) = (1.64 \pm 0.34) \times 10^{4}. \quad (1.11)$$

These decays are helicity suppressed in the SM. This is due to the necessary spin flip to account for a spin-0 particle decaying to a state of two spin-$\frac{1}{2}$ particles, introducing a proportionality to the mass of the final state fermion. This is one of the reasons the tau channel has been observed while the other two are are still only limits.

Another possible group SM-suppressed decays those involving Flavor Changing Neutral Currents(FCNC). These arise in the SM when a quark undergoes a change of flavor without changing charge, $(b \to (s, d), c \to u)$, which do not exist at tree-level in the standard model. They occur only at one loop and are thus more difficult to produce. This may be interesting because many NP theories that involve more massive particles produce effects that will only be seen at one-loop and thus can compete with SM contributions. A specific example of a FCNC process is the annihilation of a heavy meson composed of the quark pair $(b\bar{s}, b\bar{d}, c\bar{u})$, representing the mesons B_s^0, B^0, and D^0 respectively. Both leptonic and semi-leptonic final states of these decays are can constrain the effects of new physics.

1.1.4 New Physics : Dark Matter

So now we turn our attention beyond the 4.9%, baryonic, standard model, visible universe, to the remainder. There are a variety of cosmological sources that give evidence for dark matter [11, 12]. Rotational velocity distributions of galaxies [13, 14, 15], the cosmic microwave background(CMB) fluctuation spectrum [16], gravitational lensing and the evolution of large-scale cosmological structures [17] all point to a distributed density of DM that

is much larger than that of visible matter, and cannot be explained by any SM particles.

Recent efforts have been quite exhaustive theoretically to model possible scenarios of DM, and many experiments [18, 19] have been proposed, built and completed with significant results constraining the cross-sections/masses of DM candidates through direct detection.

While the presence of DM is firmly established, its basic properties are still subject of a debate. If dark matter is comprised of some fundamental particle, experimentally-measured properties, such as its relic abundance or production cross-sections can be predicted. Experimental measurements of the abundance $\Omega_{DM}h^2 \sim 0.12$ by WMAP collaboration [2] can be used to place constraints on the masses and interaction strengths of those DM particles. Indeed, the relation

$$\Omega_{DM}h^2 \sim \langle \sigma_{ann} v_{rel} \rangle^{-1} \propto \frac{M^2}{g^4}, \tag{1.12}$$

with M and g being the mass and the interaction strength associated with DM annihilation, implies that, for a weakly-interacting massive particle (WIMP) of DM, the mass scale should be set around the electroweak scale. Yet, difficulties in understanding of small-scale gravitational clustering in numerical simulations with WIMPs may lead to preference being given to much lighter DM particles. Particularly there has been interest in studying models of light dark matter particle with masses of the keV range [20, 21]. According to Eq. (1.12), the light mass of dark matter particle then implies a superweak interaction between the dark matter and standard model (SM) sector [22, 23] . Several models with light $\mathcal{O}$(keV-MeV) DM particles, or super-WIMPs, have been proposed [20, 21].

One of the main features of the super-WIMP models is that DM particles do not need to be stable against decays to even lighter SM particles [20]. This implies that one does not need to impose an ad-hoc Z_2 symmetry when constructing an effective Lagrangian for DM interactions with the standard model fields, so DM particles can be emitted and absorbed by SM particles. Due to their extremely small couplings to the SM particles, experimental searches for super-WIMPs must be performed at experiments where large statistics is available. In

addition, the experiments must be able to resolve signals with missing energy [24, 25, 26].

But before we can begin to discuss what New Physics(NP) governs these unknown sectors we must be confident that our SM calculations are both correct, and complete.

In Chapter 2 I will overview the methods and structure of the underlining models and approaches to our calculations. Chapter 3 will focus on possible contaminants to the popular rare decay channels that are currently in use for constraining new physics [27]. Chapter 4 will describe their application to constraining parameters found in two specific models of light Super-WIMP Dark Matter [28]. Chapter 5 will look at rare leptonic charm decays and possible contributions from previously uncalculated two-particle unitary intermediate states.

CHAPTER 2

FRAMEWORK FOR CALCULATIONS

2.1 Effective Field Theory

Due to the vast variety of physical phenomena it is often profitable to work in a region of energy where only certain degrees of freedom are relevant. One must then construct methods to separate out the relevant interactions from those that can be neglected for that given "scale". Usually a natural scale can be constructed from the relevant masses or interaction energies, and thus can define some small parameter in terms of which one can set up a perturbative expansion. A simple case is one of a two-particle theory with vastly separated masses; a light mass m and a heavy mass M then can be used to define your scale parameter $\Lambda = \frac{m}{M}$. It is also possible to define parameters through expansions of momenta about specific projection vectors, i.e. "collinear" and "transverse" momenta.

Using this gap between two different scales is the core of Effective Field Theory (EFT). By factorizing out physics at one scale into effective coefficients, we can parameterize a theory order-by-order in effective operators at another scale.

Operator Product Expansion

The Wilsonian [29] method of Operator Product Expansion (OPE) allows us to build a framework of effective interactions that are described by separating out the long range physical local operators and the short range, non-local Wilson coefficients.

The weak decays of hadrons are executed through the weak decay of their constituent quarks, who form a bound state through the strong interaction at energy scales roughly to order $\mathcal{O}(1GeV)$. This scale is much less than the electroweak scale, $\mathcal{O}(M_{Z,W} \approx 80 - 90GeV)$, and the strong coupling is no longer a perturbative parameter. An electroweak decay such

as $c\bar{s} \to u\bar{d}$ is mediated at tree level by the exchange of a massive W boson as seen in Figure 2.1.1.

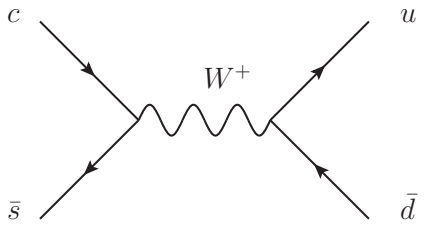

Figure 2.1.1: Leading EW Contribution to $c\bar{s} \to u\bar{d}$.

The amplitude for this diagram is

$$\mathcal{A}(c\bar{s} \to c\bar{d}) \quad = \quad \left(\frac{g}{\sqrt{2}}\right)^2 V_{cs}V_{ud}^*[\bar{s}\gamma_\mu P_L c]\frac{-i\left(g^{\mu\nu} - \frac{P^\mu P^\nu}{M_W^2}\right)}{P^2 - M_W^2}[\bar{d}\gamma_\nu P_L u], \tag{2.1}$$

where $P_L = \frac{1}{2}(1-\gamma^5)$. If we expand in powers of $\frac{P^2}{M_W^2}$ we have obtained the Fermi theory for four-quark weak interactions,

$$\mathcal{A}(c\bar{s} \to c\bar{d}) \quad = \quad i\frac{G_F}{\sqrt{2}}V_{cs}V_{ud}^*(\bar{s}c)_{V-A}(\bar{d}u)_{V-A} + \mathcal{O}(\frac{P^2}{M_W^2}), \tag{2.2}$$

where

$$(q_1\bar{q}_2)_{V-A} \quad = \quad q_1\gamma_\mu(1-\gamma^5)\bar{q}_2. \tag{2.3}$$

This is the basic idea of OPE, where a product of two currents at two different space-time points can be expanded as a series of local effective operators weighted by effective coupling constants. In this case, there is no scale-dependent coupling and so the Wilson coefficient is 1, and the W boson has been "integrated out" and is no longer a dynamical degree of freedom. The propagator connecting the two space-time points has been collapsed into a single local four-quark operator.

If we now add short distance QCD corrections we must include more operators to this effective interaction,

$$\mathcal{H}_{eff} \quad = \quad \frac{G_F}{\sqrt{2}} \sum_i V^i_{CKM} C_i(\mu^2) \mathcal{O}_i(\mu). \tag{2.4}$$

At any order the Wilson Coefficients, $C_i(\mu^2)$ can be calculated by matching the effective theory with the full theory at the given order in the perturbative expansion.

This is a method that allows the combining of higher-order interactions into lower-order effective operators to ease calculations by focusing on only the operators and coefficients specific to the concerned process.

2.1.1 Chiral Perturbation Theory (χPT)

One example of a phenomenologically successful effective field theory is Chiral Perturbation Theory (χPT) [30]. This is the application of the EFT method to QCD. While QCD is a beautiful, renormalizable theory, its applications are less that satisfactory. At very high energies asymptotic freedom allows us to calculate QCD effects perturbatively, at low energies we are faced with numerous challenges. Firstly, QCD is a theory of a *strong* interaction, meaning $\frac{g_s}{4\pi} \approx 1$ at low energies. This denies us the use of perturbative methods. Another obstacle is that experimental observables are derived from observation of QCD hadronic bound states, rather than the QCD degrees of freedom, quarks and gluons. In order to make a connection between the two one must analyze all symmetries and scales to create an effective theory with the proper behavior.

Chirality is defined through the use of projection operators, $P_{L/R} = \frac{1}{2}(1 \mp \gamma^5)$. The QCD Lagrangian can be expanded in terms of the left and right projection operators as

$$\mathcal{L}_{QCD} = \bar{q}\,(i \not{D} - m_q)\, q = \bar{q}_L i \not{D} q_L + \bar{q}_R i \not{D} q_R - \bar{q}_L m_q q_R - \bar{q}_R m_q q_L. \tag{2.5}$$

In the case of three quarks, (u, d, s), and in the massless limit $m_q \to 0$, we observe an exact $SU(3)_L \times SU(3)_R$ chiral symmetry invariance by letting

$$q_L \to g_L q_L, \quad q_R \to g_R q_R, \tag{2.6}$$

with $g_L^\dagger g_L = g_R^\dagger g_R = \mathbf{1}$. The covariant derivative is diagonal in flavor space and so

$$\bar{q}_L g_L^\dagger \not{D} g_L q_L \to \bar{q}_L \not{D} q_L. \tag{2.7}$$

The mass term

$$\bar{q}_L g_L^\dagger m_q g_R q_R - \bar{q}_R g_R^\dagger m_q g_L q_L \neq 0 \quad \forall \quad m_q \neq 0. \tag{2.8}$$

As quarks have small masses in the SM this symmetry must be broken, and this results in an octet of light pseudo-Goldstone pseudoscalar meson [31]. We are working at a scale where the momenta of these QCD effects are small compared to the large hadronic scale $\simeq 1\, GeV$, and we have the ability to expand in derivatives and masses of these pseudoscalar fields [32].

We group these pseudo-Goldstone bosons into a 3×3 matrix $\Sigma \in SU(3)$ that transforms under the chiral $SU(3)_L \otimes SU(3)_R$ as

$$\Sigma \to g_L \Sigma g_R^\dagger, \tag{2.9}$$

which is represented by

$$\Sigma = \xi^2 = exp\left(\frac{2i\pi^i \lambda^i}{f}\right), \tag{2.10}$$

where $f \approx f_\pi \approx 130$ MeV, and the sum over the 8 generators yield the hermitian and

traceless matrix

$$\pi^i\lambda^i = \begin{pmatrix} \frac{\pi^0}{\sqrt{2}} + \frac{\eta}{\sqrt{6}} & \pi^+ & K^+ \\ \pi^- & -\frac{\pi^0}{\sqrt{2}} + \frac{\eta}{\sqrt{6}} & K^0 \\ K^- & \bar{K}^0 & -\sqrt{\frac{2}{3}}\eta \end{pmatrix}. \tag{2.11}$$

From this we can begin to write an exhaustive Lagrangian for each order in both mass and momentum of the mesons. The lowest order, the kinetic term, is given by

$$\mathcal{L} = \frac{f^2}{8} Tr\left[\partial^\mu \Sigma \partial_\mu \Sigma^\dagger\right], \tag{2.12}$$

where the factor of 8 has been chosen to normalize the kinetic terms to a form similar to scalar field theory. Higher order terms appear in the expansion in momenta, $\frac{p}{\Lambda_X}$ where p is a typical momentum scale in the process and $\Lambda_X \approx 1$ GeV is the chiral symmetry breaking scale.

As defined in (2.10) $\xi(x)$ is a coset field with the chiral transformation property

$$\xi(x) \to g_L \xi(x) U^\dagger(x) = U(x)\xi(x) g_R^\dagger, \tag{2.13}$$

where $U(x)$ is a member of the $SU(3)_V$ unbroken subgroup. As this is a local, space-dependent matrix we must define covariant derivatives and gauge fields to be able to construct an invariant kinetic term and derivative couplings. This is done by the vector current definition,

$$\mathcal{V}_\mu = \frac{1}{2}\left(\xi^\dagger \partial_\mu \xi + \xi \partial_\mu \xi^\dagger\right), \tag{2.14}$$

which transforms under (2.13) as

$$\mathcal{V}_\mu \to U\mathcal{V}_\mu U^\dagger + U\partial_\mu U^\dagger. \tag{2.15}$$

We will also now define an axial current,

$$\mathcal{A}_\mu = \frac{i}{2}\left(\xi^\dagger\partial_\mu\xi - \xi\partial_\mu\xi^\dagger\right), \tag{2.16}$$

that transforms as

$$\mathcal{A}_\mu \to U\mathcal{V}_\mu U^\dagger. \tag{2.17}$$

We can now introduce electromagnetic interactions, a $U(1)$ symmetry, with the covariant derivative definition

$$\mathcal{D}_\mu\xi = \partial_\mu\xi + ieB_\mu[Q,\xi], \tag{2.18}$$

where $Q = diag(\frac{2}{3}, -\frac{1}{3}, -\frac{1}{3})$.

As we have mentioned, the chiral symmetry is not exact, and is broken by the quark mass term

$$\sum_{i=u,d,s} \bar{q}_i\hat{m}_{ij}q_j, \tag{2.19}$$

where m_{ij} is the light mass matrix

$$\hat{m}_{ij} \quad = \quad \begin{pmatrix} m_u & 0 & 0 \\ 0 & m_d & 0 \\ 0 & 0 & m_s \end{pmatrix}. \tag{2.20}$$

This breaking can be implemented at first order in the quark masses by the additional term

$$\mathcal{L}_{\hat{m}} \quad = \quad \lambda_0 Tr\left(\hat{m}\Sigma + \Sigma^\dagger \hat{m}\right) + \mathcal{O}(\hat{m}^2). \tag{2.21}$$

This breaking leads to the different masses of the octet mesons as well as additional contributions to relevant form factors.

This completes our building blocks of the light portion of our effective theory, and we can write our LO Lagrangian in derivatives and mass

$$\mathcal{L}_{LO} \quad = \quad \frac{f^2}{8} D\mu\Sigma_{ab} D^\mu \Sigma^\dagger_{ba} + \lambda_0 Tr\left(\hat{m}\Sigma + \Sigma^\dagger \hat{m}\right) + \mathcal{O}((\partial\Sigma)^3) + \mathcal{O}(\hat{m}^2). \tag{2.22}$$

Here we have set up a method of expanding the effective Lagrangian in powers of the chiral momenta, $\partial\Sigma$ as well as the symmetry-breaking mass terms $\hat{m}$. Contributions from the leading order Lagrangian with chiral loops can be considerable, and must be checked for validity when performing both expansions. It should be noted that it is often acceptable when performing to perform calculations at leading order and one loop without explicit quark-mass corrections, but rather substituting the relevant masses and form factors. This completes our leading order description of the soft portion of our effective theory.

2.1.2 Heavy Quark/Meson Effective Theory

Another natural scale appearing in the standard model is the ratio of Λ_{QCD} to the mass of the heavy quarks, $\mu = \frac{\Lambda_{QCD}}{m_Q}$. Using this as our expansion parameter one can expand to obtain a theory describing the heavy quarks at leading order as static gluon sources, rather than dynamical degrees of freedom [33]. This is similar to a static proton in the hydrogen atom. In the limit of $m_Q \to \infty$ the heavy quark spin decouples from the gluon field. This means that it can be rotated from a $0^- \to 1^-$ state without changing the physics. In this limit the two states would also be degenerate in mass and have identical properties. Allowing

some large mass M the hyperfine splitting between the spin states will be $\mathcal{O}(\Lambda_{QCD}^2/M)$. We can take advantage of this spin freedom to develop many relations between the heavy-hadron form factors, simplifying phenomenological calculations greatly [33].

If we consider a meson H composed of one heavy(c or b) and one light(u, d, s) quark, $\bar{Q}q$, we can factor the heavy quark momenta into both static and dynmaic parts as [34],

$$p_Q = m_Q v + k, \tag{2.23}$$

where k is the residual momentum of the order Λ_{QCD}. We can extract the heavy part of the field through the redefinition into small and large respective components

$$Q_v(x) = exp(im_Q vx)Q(x) = h_v(x) + H_v(x), \tag{2.24}$$

where the small component H is $\mathcal{O}(1/m_Q)$. These field satisfy the projections

$$\not{v} H_v = -H_v, \qquad \not{v} h_v = h_v. \tag{2.25}$$

At tree-level one simply plugs in the new field and solves the equation of motion for the light field H. Reinserting into the lagrangian we obtain after some algebra and an expansion in $1/m_Q$ the tree-level kinetic term

$$\mathcal{L}^{(0)} = \bar{h}_v \left(iv \cdot D\right) h_v. \tag{2.26}$$

This decomposition is not unique, as we can reparameterize the momenta definition (2.23) as

$$v \to v + \frac{q}{m_Q}, \qquad k \to k - q, \tag{2.27}$$

where $v \cdot q = 0$ to have $v^2 = 1$, must yield the same physical observables. This provides a constraint on the coefficients of the next-order lagrangian terms, as they must maintain this reparameterization invariance.

We now construct physical states using the above mentioned symmetries. It is common use and well defined in literature to use the matrix representation for the spin-degenerate negative parity doublet

$$H_a = \frac{1+\not{v}}{2}(P^*_{a\mu}\gamma^\mu - P_a\gamma_5), \qquad \bar{H}_a = \gamma^0(H_a)^\dagger\gamma^0, \tag{2.28}$$

to describe the heavy meson pseudoscalar and vector fields. Here the indices a nd b reflect the light quark flavor indices, v is the velocity of the heavy quark and the P can be either a B or D meson. The operators P satisfy the normalization conditions

$$\langle 0|P_q|Q\bar{q}(0^-)\rangle = \sqrt{M_H}, \qquad \langle 0|P^{*\mu}_q|Q\bar{q}(1^-)\rangle = \epsilon^\mu\sqrt{M_H},$$

where M_H is the mass of the heavy meson in question.

As the heavy meson is composed of one heavy quark $Q = (Q_c, Q_b)$ and one light quark $q_a = (q_u, q_d, q_s)$, the field H_a transforms as $\bar{3}$ under the chiral transformation, such that $H_a \to H_b U^\dagger_{ba}$, where U was seen in (2.13).

2.1.3 Heavy Meson Chiral Perturbation Theory

Knowing the transformation properties of both the light and heavy fields we can now construct all C,P,T and Lorentz invariant lagrangians at a given order in $1/M$, the mass of the heavy meson.

The leading order lagrangian is [30]

$$\mathcal{L}_{(0)} = iTr\left[H_b v\cdot D_{ba}\bar{H}_a\right] + igTr\left[H_b\gamma_\mu\gamma^5\mathcal{A}^\mu_{ba}\bar{H}_a\right] + \frac{f^2}{8}D_\mu\Sigma_{ab}D^\mu\Sigma^\dagger_{ba}. \tag{2.29}$$

This leads to the propagator for both P and P^* to be $\frac{i}{2v\cdot k}$. The NLO contribution from the $1/M$ expansion is

$$\begin{aligned}\mathcal{L}_{1/M} &= \frac{\lambda_2}{M} Tr[\bar{H}_a \sigma_{\mu\nu} H_a \sigma^{\mu\nu}] \\ &+ \frac{g_1}{M} Tr\left[H_b \gamma_\mu \gamma^5 \mathcal{A}^\mu_{ba} \bar{H}_a\right] \\ &+ \frac{g_2}{M} Tr\left[\gamma_\mu \gamma^5 \mathcal{A}^\mu_{ba} H_b \bar{H}_a\right].\end{aligned} \tag{2.30}$$

These will lead to corrections to the leading order constant g for VV and PV interactions,

$$\begin{aligned} g \to g_{P^*P^*} &= g + \frac{1}{M}(g_1 + g_2) \\ g \to g_{PP^*} &= g + \frac{1}{M}(g_1 - g_2). \end{aligned} \tag{2.31}$$

Additionally, if we define $\lambda_0 = -M\Delta/2 = -M/2(M_{P^*} - M_P)$ we see a shift of the respective P and P^* propagators,

$$\frac{i}{2(v\cdot k + \frac{3}{4}\Delta)}, \qquad \frac{-i\left(g^{\mu\nu} - v^\mu v^\nu\right)}{2(v\cdot k - \frac{1}{4}\Delta)} \tag{2.32}$$

We can also now incorporate an interaction with the previously introduce $U(1)$ electromagnetic gauge boson, with the definition

$$D^\mu_{ab} H_b = \partial^\mu H_a + ieB^\mu \left(Q'_Q H - HQ\right)_a - H_b \mathcal{V}^\mu_{ab} H_b, \tag{2.33}$$

having now defined $Q'_Q = (\frac{2}{3}, -\frac{1}{3})$ depending on the flavor of the heavy quark. Following [35] we also introduce a contact term

$$\mathcal{L}_\beta = -\frac{\beta e}{4} Tr\left[H_b \sigma^{\mu\nu} F_{\mu\nu} Q^\xi_{ba} \bar{H}_a\right] - \frac{e}{4m_Q} Q'_Q Tr\left[\bar{H}_a \sigma^{\mu\nu} H_a F_{\mu\nu}\right], \tag{2.34}$$

where $Q^\xi = \frac{1}{2}\left(\xi^\dagger Q \xi + \xi Q \xi^\dagger\right)$. The first term describes the interaction of the photon with

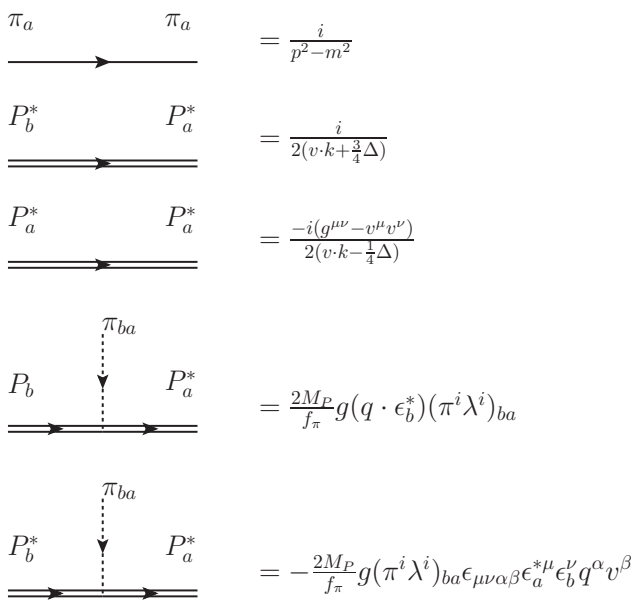

Figure 2.1.2: Feynman Rules for HMχPT

the light degrees of freedom contained inside of the heavy meson, while the second term describes the interaction with the heavy quark, and is therefor suppressed by $1/m_Q$. Though this is suppressed at leading order, we will see that it is actually important when considering certain transitions, as it can have cancellation effects with one-loop corrections to transition amplitudes.

Our leading order Lagrangian with the electromagnetic interaction is thus the combination of (2.34) and (2.29). This gives us the following Feynman diagrams for the interaction between the heavy and chiral meson fields in Figure 2.1.2.

2.1.4 Unitary Conditions

In order to maintain conservation of probability the Hamiltonian should be Hermetian, $H^\dagger = H$. This implies that the S-matrix is unitary[36],

$$S^\dagger S = 1. \tag{2.35}$$

An implication of this condition is what is known as the optical theorem. Given the S-matrix as

$$S = \mathbf{1} + iT, \tag{2.36}$$

we recall that Feynman diagrams are elements of this transition matrix defined as

$$\langle f|T|i\rangle = (2\pi)^4 \delta^4 \left(p_i - p_f\right) \mathcal{M}(i \to f). \tag{2.37}$$

We can now show a very useful relation,

$$\mathbf{1} = S^\dagger S = (1 - iT^\dagger)(1 + iT) = 1 - i(T^\dagger - T) + T^\dagger T, \tag{2.38}$$

$$\Rightarrow i(T^\dagger - T) = T^\dagger T. \tag{2.39}$$

Applying initial and final states, and on the right hand side inserting a complete set of states and integrating over the Lorentz-invariant phase space (LIPS) we arrive at

$$\langle f|i(T^\dagger - T)|i\rangle = \sum_X \int d\Pi^X_{LIPS} \langle f|T^\dagger|X\rangle\langle X|T|i\rangle. \tag{2.40}$$

This implies, from our original unitary condition, the Generalized Optical Theorem

$$\mathcal{M}(i \to f) - \mathcal{M}(f \to i)^\dagger = i \sum_X \int d\Pi^X_{LIPS} (2\pi)^4 \delta^4 \left(p_i - p_f\right) \mathcal{M}(i \to X)\mathcal{M}(X \to f)^\dagger. \tag{2.41}$$

Assuming Time reversal invariance, this implies [36]

$$\mathcal{M}(i \to f) - \mathcal{M}(f \to i)^\dagger = 2\mathcal{I}m\mathcal{M}(i \to f). \tag{2.42}$$

Thus the imaginary part of the intermediate-state contribution will be part of the final amplitude.

2.1.5 Cutting Rules and Dispersion Relations

Cauchy's integral theorem provides that given the imaginary part of a complex function and knowledge of the function behavior at infinity, one can reconstruct the entire function using a suitable dispersion relation(DR). This is particularly useful as given an amplitude containing loops one can directly calculate the imaginary part of the amplitude at an arbitrary invariant mass, s, by means of Cutkosky's rule [37], which is a result of unitarity.

We can construct a DR by considering some complex function, $f(s)$, where s is complex. Assuming that $\forall\, s < m^2 : f(s) \in \mathbb{R}$, $f(s)$ has a branch cut for real $s > M^2$, and $f(s) \in \mathbb{C}$ everywhere else, we can show, with the use of Schwartz's reflection principle, that

$$\begin{aligned} f(s+i\epsilon) &= Re[f(s)] + iIm[f(s)], \qquad \epsilon > 0 \\ f(s-i\epsilon) &= Re[f(s)] - iIm[f(s)], \qquad \epsilon > 0 \end{aligned} \tag{2.43}$$

This implies

$$f(s+i\epsilon) + f(s-i\epsilon) = 2iIm[f(s)]. \tag{2.44}$$

We now employ Cauchy's theorem,

$$\begin{aligned} f(M^2) &= \frac{1}{2\pi i}\oint_{\mathbb{C}} ds \frac{f(s)}{s-M^2}, \\ &= \frac{1}{2\pi i}\left(\int_{m^2}^{\infty} ds \frac{f(s+i\epsilon)+f(s-i\epsilon)}{s-M^2} + \oint_{|s|=\infty} ds \frac{f(s)}{s-M^2}\right), \\ &= \frac{1}{\pi}\int_{m^2}^{\infty} ds \frac{Im[f(s)]}{s-M^2-i\epsilon} + \frac{1}{2\pi i}\oint_{|s|=\infty} ds \frac{f(s)}{s-M^2}. \end{aligned} \tag{2.45}$$

If the limit on the edge of the contour vanishes at infinity we are left with the unsubtracted DR,

$$f(M^2) \quad = \quad \frac{1}{\pi}\int_{m^2}^{\infty} ds \frac{Im[f(s)]}{s - M^2 - i\epsilon}. \tag{2.46}$$

It is easy to show, using the relation

$$\int_s \frac{g(s)}{1 - s \pm i\epsilon} = \mathbb{P}\left[\int_s \frac{g(s)}{1-s}\right] + \mp i\pi \int_s g(s)\delta(1-s), \tag{2.47}$$

where $\mathbb{P}$ is the Principal Value of the integrand, that the real part of $f(s)$ is

$$Re[f(s)] \quad = \quad \frac{1}{\pi}\mathbb{P}\int_{m^2}^{\infty} ds \frac{Im[f(s)]}{s - M^2}. \tag{2.48}$$

Unfortunately, when dealing with SM loop calculations, the behavior at ∞ does not always tend to zero on the contour. The integral can still be performed by subtracting from (2.45) the function at some real point $q_0^2 < m^2$,

$$\begin{aligned} f(M^2) \quad = \quad & f(q_o^2) + \frac{M^2 - q_0^2}{\pi}\int_{m^2}^{\infty} \frac{ds}{s - q_0^2}\frac{Im[f(s)]}{s - M^2 - i\epsilon} \\ & + \frac{M^2 - q_0^2}{2\pi i}\oint_{|s|=\infty} \frac{f(s)}{(s - q_0^2)(s - M^2)}. \end{aligned} \tag{2.49}$$

If the boundary integral vanishes, we have the once-subtracted dispersion relation,

$$f(M^2) \quad = \quad f(q_o^2) + \frac{M^2 - q_0^2}{\pi}\int_{m^2}^{\infty} \frac{ds}{s - q_0^2}\frac{Im[f(s)]}{s - M^2 - i\epsilon}. \tag{2.50}$$

This method of subtraction can be used multiple times to regularize the boundary integral.

CHAPTER 3

FAKING $B_s^0 \to \mu^+\mu^-$

This work was published in reference [27].

3.1 Introduction

The rare leptonic decay of the B_s^0 into a dimuon pair, $B_s^0 \to \mu^+\mu^-$, is an example of a flavor-changing neutral current (FCNC) process. Studies of such decay processes not only play an important role in determining electroweak and strong interaction parameters of the standard model (SM) of particle physics, but also serve as sensitive probes of possible physics beyond the standard model [38]. While recent evidence for observation of $B_s^0 \to \mu^+\mu^-$ from LHC-b collaboration, as well as an earlier result from CDF [39] preclude any spectacular new physics (NP) effect, there is still room for NP to influence this decay. It is then important to have a firm evaluation of $\mathcal{B}(B_s^0 \to \mu^+\mu^-)$ in the SM [40, 41] and a firm understanding that the experimentally-observed branching ratio

$$\begin{aligned} \mathcal{B}_{LHCb}(B_s^0 \to \mu^+\mu^-) &= (3.2^{+1.5}_{-1.2}) \times 10^{-9} \\ \mathcal{B}_{CDF}(B_s^0 \to \mu^+\mu^-) &= (1.8^{+1.1}_{-0.9}) \times 10^{-8} \end{aligned} \tag{3.1}$$

actually corresponds to the $B_s^0 \to \mu^+\mu^-$ transition.

It is well known that the $B_s^0 \to \mu^+\mu^-$ decay is helicity suppressed in the SM by $m_\mu^2/m_{B_s}^2$ due to the left handed nature of weak interactions [42]. This effect arises from the necessary spin flip on the outgoing back-to-back lepton pair in order to conserve angular momentum since the initial state meson is spinless.

This suppression is absent in B_s^0 decays where the muon pair is produced with one or more additional particles in the final state that can carry away a unit of angular momentum,

such as $B_s^0 \to \mu^+\mu^-\gamma$ or $B_s^0 \to \mu^+\mu^-\nu_\mu\bar{\nu}_\mu$. This means that, in general, those processes could have sizable total branching ratios, comparable to that of $B_s^0 \to \mu^+\mu^-$, despite being suppressed by other small parameters (such as α_{EM} for $B_s^0 \to \mu^+\mu^-\gamma$) [43]. If, in addition, the final state photon or $\nu\bar{\nu}$ is undetected, while the invariant mass of $\mu^+\mu^-$ pair is close to $m_{B_s^0}$, then the experimentally-measured branching ratio would correspond to

$$\mathcal{B}_{exp}(B_s^0 \to \mu^+\mu^-) = \mathcal{B}(B_s^0 \to \mu^+\mu^-)\left[1 + \sum_X \frac{\mathcal{B}(B_s^0 \to \mu^+\mu^- X)|_{m(\mu^+\mu^-)\approx m_{B_s})}}{\mathcal{B}(B_s^0 \to \mu^+\mu^-)}\right], \qquad (3.2)$$

where X is an undetected particle or a group of particles. The contribution of $B_s^0 \to \mu^+\mu^- X$ would depend on how well X could be detected in a particular experiment, as well as on whether $B_s^0 \to \mu^+\mu^- X$ has any kind of resonance enhancement that is not well modeled by background models chosen by a particular experiment in a given window of $m(\mu^+\mu^-)$, as well as the size of that window. For example, for $X = \gamma$, most current searches use di-lepton energy cuts that would correspond to an allowable soft photon of up to 60 MeV[1]. For $B \to \ell\nu_\ell$ transition and $X = \gamma$ similar effects were discussed in [44, 45, 46], and for X being light particles – in [28]. In the following we shall concentrate on the amplitudes that are non-vanishing in the $m_\mu \to 0$ limit.

3.2 $B_s^0 \to \mu^+\mu^-\gamma$ transition

Due to higher backgrounds in hadron collider experiments soft photons emitted in $B_s^0 \to \ell^+\ell^-\gamma$ could be hard to detect, so this background could be quite important. These decays were previously analyzed in [43, 47, 48, 49, 50], where multiple models have been considered. The analysis presented in [43] was mainly geared towards kinematical regimes where the photon is sufficiently hard to be detected; in fact, low-energy cut-offs were introduced on photon energies. Similarly, perturbative QCD-related approaches of [47, 48, 49, 50] cannot

[1]This cut would almost exclude the possibility of missing a π^0 or heavier neutral particles.

adequately describe the soft photon region. In this paper, we apply a model-independent approach that incorporates both heavy quark symmetry for hadrons containing a heavy quark with mass $m_Q >> \Lambda_{QCD}$, and chiral $SU(3)_L \times SU(3)_R$ symmetries in the $m_q \to 0$ limit [51, 52] suited for this kinematical region. We organize our calculations in terms of an expansion in $1/m_b$ and examine the contribution of terms up to leading order in $\mathcal{O}(1/m_b)$.

Similarly to $B \to \ell\nu_\ell\gamma$ [45], the decay amplitude for $B_s \to \mu^+\mu^-\gamma$ transition can be broken into two generic parts containing internal bremsstrahlung (IB) and structure dependent (SD) contributions. The bremsstrahlung contributions are still helicity suppressed, while the SD contribution contain the electromagnetic coupling α but are not suppressed by the lepton mass. Phenomenologically, the origin of that can be understood as follows. When the soft photon in emitted from the B_s meson, heavy intermediate states including the $J^P = 1^-$ B_s^* vector meson state become possible. This lifts helicity suppression since the lepton pair couples directly to the spin 1 meson. In the kinematic regime where the photon is soft, we expect that significant contribution comes only from the vector B_s^* resonance for reasons analogous to the B^* pole dominance in $B \to \pi\ell\nu$ at near zero pionic recoil energies [53]: in the large m_b limit the B_s^* and B_s become degenerate and the residual mass splitting is $m_{B^*} - m_B \sim \mathcal{O}(1/m_b)$ [54]. Therefore, excitation of the B_s^* does not require much energy. There are two diagrams containing an intermediate B_s^* as seen in Fig. 3.2.1. In the kinematic region of interest where $E_\gamma < 60$ MeV, Fig. 3.2.1 (b) is neglected. This can be easily seen considering it is a contribution from an off-shell intermediate B_s^* that decays to an on-shell soft photon in a vector-meson-dominance fashion via $b \to s\gamma$ transition. Since the photon is on mass shell, the B_s propagator makes it $(1/M_{B_s^0}^2)$ suppressed. In the effective field theory language this diagram corresponds to a higher-dimensional operator whose contribution is suppressed by powers of M_B. Similarly, a contribution of Fig. 3.2.1 (c) is also $(1/M_{B_s^0}^2)$, so it too will be neglected in what follows.

The calculation of soft photon effects should carefully deal with soft divergences. Those

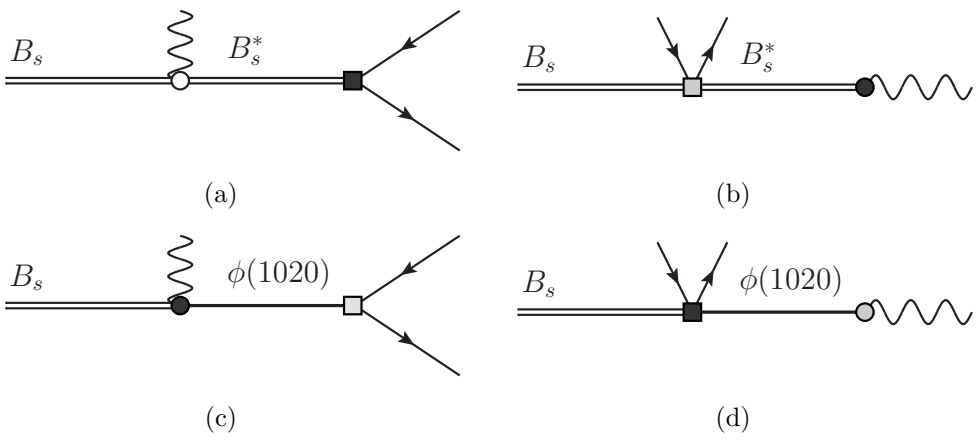

Figure 3.2.1: Resonant contributions to $B_s \to \mu^+\mu^-\gamma$. The dark grey vertices represent the $b \to s$ effective Hamiltonians in Eqs. (3.10, 3.15). Light grey vertices are SM neutral currents while the white circle in (a) is defined in Eq. (3.4).

are canceled between one-loop radiative corrections to $B_s \to \mu^+\mu^-$ and $B_s \to \mu^+\mu^-\gamma$.

We employ Heavy Meson Chiral Perturbation Theory (HMχPT) to calculate Fig. 3.2.1 (a).

To evaluate diagram Fig. 3.2.1 (a) we need an amplitude for a $B \to B^*\gamma$ transition as

$$\mathcal{M}_{[B_s \to B_s^* \gamma_s \to \mu^+\mu^-\gamma_s]} = \mathcal{M}^{\mu}_{B_s^* \to \mu^+\mu^-} \times \frac{g_{\mu\alpha}}{M^2_{B_s^*}} \times \mathcal{M}^{\alpha}_{B_s \to B_s^*\gamma}, \tag{3.3}$$

The amplitude for $B \to B^*\gamma$ is conventionally parameterized as

$$\mathcal{M}_{B_s \to B_s^*\gamma} = -ie\mu\eta^*_\alpha v_\beta k_\mu \epsilon^*_\nu \epsilon^{\mu\nu\alpha\beta}, \tag{3.4}$$

where k is the 4-momentum of the photon, v the velocity of the decaying heavy meson, η is the vector meson polarization, and ϵ is the photon polarization. The strength of the transition is described by the magnetic moment, μ, which receives contributions from the photon coupling to both heavy and the light quark components of the electromagnetic current [55],

$$\mu = \mu_b + \mu_\ell. \tag{3.5}$$

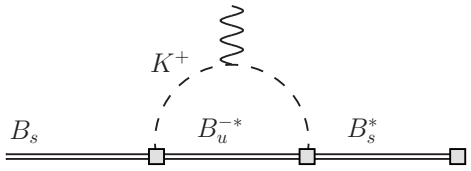

Figure 3.2.2: One loop corrections to magnetic moment μ. The double lines denote the heavy mesons B and B^* while the single line denotes the goldstone bosons

The bottom quark contribution is fixed by heavy quark symmetry to be $\mu_b = Q_b/m_b = -1/(3m_b)$, while the light quark contribution can be computed, to one loop, in HMχPT. The relevant effective Lagrangian is [35, 55]

$$\mathcal{L}_\beta = \frac{\beta e}{4}\mathrm{Tr}(\bar{H}_a H_b \sigma^{\mu\nu} F_{\mu\nu} Q^\xi_{ba}) + \frac{ig}{2}\,\mathrm{Tr}\left(\bar{H}_a H_b \gamma_\mu \gamma_5 (\xi^\dagger \partial^\mu \xi - \xi \partial^\mu \xi^\dagger)_{ba}\right), \tag{3.6}$$

where Tr is a trace over the Dirac indices, and β is a coupling constant parameterizing a local contribution to the light quark magnetic moment. We include the most important one-loop correction, which is shown in Fig. 3.2.2.

The effective magnetic moment for the $B_s \to B_s^*\gamma$ transition is then

$$\mu_{B_s\gamma} = -\frac{1}{3m_b} - \frac{1}{3}\beta + g^2 \frac{m_K}{4\pi f_K^2}, \tag{3.7}$$

where g is the χPT coupling constant, and m_K, f_K are the mass and decay constant of the Kaon respectively. The constants β and g can be extracted from a combination of the experimental D^{*+} branching ratios, $\mathcal{B}(D^{*+} \to D^+\gamma) = 0.016 \pm 0.004$ and $\mathcal{B}(D^{*+} \to D^0\pi^+) = 0.677 \pm 0.005$, and the total width, where the newest preliminary result from BaBar collaboration is reported to be $\Gamma_{D^{*+}} = 83.5 \pm 1.7 \pm 1.2$ KeV [56]. The decay widths

for these processes using the method above are given by

$$\Gamma(D^{*+} \to D^+\gamma) = \frac{\alpha_{EM}}{3}\left(\frac{2}{3m_c} - \frac{1}{3}\beta + g^2\frac{m_\pi}{4\pi f_\pi^2}\right)^2 |\vec{k}|^3, \tag{3.8}$$

$$\Gamma(D^{*+} \to D^0\pi^+) = \frac{g^2}{6\pi f_\pi^2}|\vec{p_\pi}|^3. \tag{3.9}$$

This yields the approximate values of the coupling constants, $g \approx 0.552$ and $\beta \approx 7.29 GeV^{-1}$. With Eq.3.7 this gives us $|\mu_{eff}| \approx 1.13$ GeV^{-1}.

To complete evaluation of Fig. 3.2.1 (a) in Eq. (3.3), we evaluate the $B_s^* \to \mu^+\mu^-$ transition. The effective Hamiltonian describing the weak $b \to s\ell^+\ell^-$ transition is

$$\begin{aligned}\mathcal{H}_{b\to s\bar{\ell}\ell} = \frac{G_F}{\sqrt{2}}V_{tb}V_{ts}^*\frac{e^2}{8\pi^2}\Big[\bar{s}\gamma^\mu(1 &- \gamma_5)b\cdot\bar{\ell}\left[C_{9V}^{eff}(\mu,q^2)\gamma_\mu + C_{10A}(\mu^2)\gamma_\mu\gamma_5\right]\ell \\ &- 2im_b\frac{C_{7\gamma}(\mu^2)}{q^2}q_\nu\cdot\bar{s}\sigma^{\mu\nu}(1+\gamma_5)b\cdot\bar{\ell}\gamma_\mu\ell\Big],\end{aligned} \tag{3.10}$$

where $q_\nu = (p_{\ell^+} + p_{\ell^-})_\nu$ is the momentum of the lepton pair and C_i are scale-dependent Wilson coefficients. The matrix element for $B_s^* \to \mu\bar{\mu}$ is then

$$\begin{aligned}\mathcal{M}_{B_s^*\to\mu^+\mu^-} = i\frac{G_F}{\sqrt{2}}V_{tb}V_{ts}^*\frac{e^2}{8\pi^2}f_{B_s}M_{B_s}\Big[&\eta_\mu^*\bar{u}(p_{\mu^+})[C_9\gamma^\mu + C_{10}\gamma^\mu\gamma_5]v(p_{\mu^-}) \\ - &2m_b\frac{C_7}{q^2}(\bar{u}(p_{\mu^+})\gamma_\mu v(p_{\mu^-}))q_\nu(i\epsilon^{\mu\nu\alpha\beta}v_\alpha\eta_\beta + v^\mu\eta^\nu - v^\nu\eta^\mu)\Big],\end{aligned} \tag{3.11}$$

where η^μ and v^μ are the polarization and 4-velocity of the vector meson respectively. We defined $\langle 0|\bar{s}_L\gamma^\mu b_L|B_s^*\rangle = \eta^\mu f_{B_s^*}/2$, and $\langle 0|\bar{s}\sigma^{\mu\nu}(1+\gamma_5)b|B_s^*\rangle = M_B f_{B_s}[i\epsilon^{\mu\nu\alpha\beta}v_\alpha\eta_\beta + v^\mu\eta^\nu - v^\nu\eta^\mu]$, with $f_{B_s^*} = M_{B_s}f_{B_s}$ [30]. This gives for the amplitude of Fig. 3.2.1 (a)

$$\begin{aligned}\mathcal{M}_{[B_s\to B_s^*\gamma_s\to\mu^+\mu^-\gamma_s]} = &\frac{G_F}{\sqrt{2}}V_{tb}V_{ts}^*\frac{e^3}{8\pi^2}\mu_{eff}\frac{f_{B_s}}{q^2 - M_{B_s^*}^2}\left(\epsilon^{\mu\nu\alpha\beta}\epsilon_\mu^* k_\alpha q_\beta\right) \\ \times &\Big[\left(2C_7m_b - C_9M_{B_s^*}\right)[\bar{u}_{p_1}\gamma_\nu v_{p_2}] - C_{10}M_{B_s^*}[\bar{u}_{p_1}\gamma_\nu\gamma_5 v_{p_2}]\Big].\end{aligned} \tag{3.12}$$

The other contribution that is leading the $M_{B_s} \to \infty$ limit is given in Fig. 3.2.1 (c)

$$\mathcal{M}_{[B_s^0 \to \mu\bar{\mu}\phi \to \mu\bar{\mu}\gamma_s]} = \mathcal{M}_{B_s^0 \to \mu\bar{\mu}\phi} \times \frac{g_{\mu\nu}}{m_\phi^2} \times \mathcal{M}_{\phi \to \gamma_s}, \tag{3.13}$$

Employing vector-meson dominance, and using the definition of the vector meson decay constant $\langle 0|\bar{s}\gamma^\mu s|\phi\rangle = f_\phi m_\phi \eta_\phi^\mu$, where η_ϕ^μ is the polarization of the ϕ meson, and $\langle\gamma|\bar{s}(-ieQ_s \not{A})s|\phi\rangle = (-ieQ_s)\epsilon_\mu^* \langle 0|\bar{s}\gamma^\mu s|\phi\rangle$,

$$\mathcal{M}^\mu_{\phi\to\gamma_s} = \frac{1}{3}\, e\, f_\phi\, m_\phi\, \epsilon_\mu^*. \tag{3.14}$$

Again, we calculate $\mathcal{M}_{B_s^0 \to \mu\bar{\mu}\phi}$ using (HMχpT). For the short distance contributions we use the effective Hamiltonian describing $b \to s\bar{\ell}\ell$ transitions in Eq. 3.10, as well as the effective Hamiltonian for $b \to s\gamma$,

$$\mathcal{H}_{b\to s\gamma} \;=\; \frac{G_F}{\sqrt{2}} V_{tb} V_{ts}^* \frac{e}{8\pi^2} m_b C_{7\gamma}(\mu^2) \cdot \bar{s}\sigma^{\mu\nu}(1+\gamma_5) b \cdot F_{\mu\nu}. \tag{3.15}$$

In order to bosonize the quark currents found in Eqs. (3.10) and (3.15) we introduce the light vector octet to the HMχpT [30],

$$\rho_\mu \equiv i\frac{g_V}{\sqrt{2}} \begin{pmatrix} \frac{\rho^0}{\sqrt{2}} + \frac{\omega}{\sqrt{2}} & \rho^+ & K^{*+} \\ \rho^- & -\frac{\rho^0}{\sqrt{2}} + \frac{\omega}{\sqrt{2}} & K^{*0} \\ K^{*-} & \bar{K}^{*0} & \phi \end{pmatrix}. \tag{3.16}$$

The bosonized currents $\bar{s}\gamma^\mu(1-\gamma_5)b$ and $\bar{s}\sigma^{\mu\nu}(1+\gamma_5)b$ are, respectively,

$$\begin{aligned} L^\mu_{1a} &= \alpha_1 \langle \gamma_5 H_b (\rho^\mu)_{bc} \xi^\dagger_{ca} \rangle, \\ L^{\mu\nu}_{1a} &= i\alpha_1 \left\{ g^{\mu\alpha} g^{\nu\beta} - \frac{i}{2}\epsilon^{\mu\nu\alpha\beta} \right\} \langle \gamma_5 H_b [\gamma_\alpha (\rho_\beta)_{bc} - \gamma_\beta (\rho_\alpha)_{bc}] \xi^\dagger_{ca} \rangle. \end{aligned} \tag{3.17}$$

A numerical value of $\alpha_1 = -0.07\,GeV^{1/2}$ [30] will be used for our calculations. Keeping only the gauge invariant portion, the amplitude for the decay with an intermediate $\phi(1020)$ is

$$\begin{aligned}\mathcal{M}_{[B_s^0\to\mu\bar{\mu}\phi\to\mu\bar{\mu}\gamma_s]} &= G_F V_{tb}V_{ts}^* \frac{e^3 f_\phi g_\phi \alpha_1 C_7 m_b}{24\pi^2\sqrt{M_{B_s}} m_\phi (p_1\cdot p_2)} \epsilon_\mu^* \Big((k\cdot(p_1+p_2))[\bar{u}_{p_1}\gamma^\mu v_{p_2}] \\ &- (p_1+p_2)^\mu [\bar{u}_{p_1} \not{k} v_{p_2}] + i\epsilon^{\mu\nu\alpha\beta} k_\alpha (p_1+p_2)_\beta [\bar{u}_{p_1}\gamma_\nu v_{p_2}] \Big). \end{aligned} \tag{3.18}$$

We checked that other contributions to the decay are smaller then the ones considered above. We considered the bremsstrahlung diagrams where a soft photon is emitted from one of the outgoing leptons. These diagrams will result in an infrared divergence in the soft region, which has been shown to cancel with the 1-loop QED vertex corrections [57]. The vertex corrections, as well as the bremsstrahlung contributions, will remain suppressed by a power of the lepton mass. Therefore the remaining non-divergent contributions from both the bremsstrahlung and vertex corrections to final states with either an electron or a muon would not be significant.

The only contribution to the amplitude from the effective Hamiltonian describing the weak transition in Eq.(3.10) ends up being the $\mathcal{O}_{10}$ operator. This comes from obtaining the matrix elements for the pseudoscalar meson,

$$\langle 0|(\bar{s}\gamma^\mu(1-\gamma_5)b)|B_s\rangle = -if_B P_B^\mu, \tag{3.19}$$

$$\langle 0|(\bar{s}\sigma^{\mu\nu}(1+\gamma_5)b)|B_s\rangle = 0, \tag{3.20}$$

where f_B is the decay constant of the B meson. With these definitions and using the conservation of the vector current we can arrive at an expression for the amplitude

$$\mathcal{M}_{Brem} = ie\frac{\alpha_{EM}G_F}{2\sqrt{2}} V_{tb}V_{ts}^* f_B C_{10} m_\mu \left[\bar{\mu}\left(\frac{\not{\epsilon}\not{P}_B}{p_{\mu^-}\cdot k} - \frac{\not{P}_B\not{\epsilon}}{p_{\mu^+}\cdot k}\right)\gamma_5\mu\right], \tag{3.21}$$

where ϵ^μ and k are the polarization and momentum of the photon respectively. Just as

we would expect from the helicity structure involved, the amplitude for the bremsstrahlung contribution is proportional to the lepton mass. So in the limit $m_\ell \to 0$, this contribution should be small compared to the non helicity-suppressed contributions.

Each amplitude from Eqs. (3.12, 3.18, 3.21) individually satisfy the Ward identity and are thus independently gauge invariant. Putting everything together, the distribution of the decay width as a function of the kinematic variable $s = (P_{B_s} - k)^2/M_{B_s}^2 = q^2/M_{B_s}^2$, in the limit $m_\ell \to 0$,

$$\frac{d\Gamma}{ds} = \left.\frac{d\Gamma}{ds}\right|_{B_s^*} + \left.\frac{d\Gamma}{ds}\right|_{\phi B_s^*} + \left.\frac{d\Gamma}{ds}\right|_{\phi}, \tag{3.22}$$

where the decay distributions are given for the two different resonance amplitudes and their interference.

$$\begin{aligned}
\frac{d\Gamma}{ds}|_{B_s^*} &= X_{CKM} M_{B_s}^3 f_{B_s}^2 \mu_{eff}^2 \left[(|C_9|^2 + |C_{10}|^2) x_{B_s^*} + 4\, C_7^2 x_b - 4\, C_7 C_9 x_b x_{B_s^*}\right] \frac{s(1-s)^3}{(s - x_{B_s^*}^2)^2}, \\
\frac{d\Gamma}{ds}|_{\phi} &= X_{CKM} \left[\frac{16\, C_7^2\, f_\phi^2\, g_\phi^2\, m_b^2\, \alpha_1^2}{9\, m_\phi^2}\right] \frac{(1-s)^3}{s}, \\
\frac{d\Gamma}{ds}|_{\phi B_s^*} &= X_{CKM} \left[\frac{4\sqrt{2} f_{B_s} f_\phi g_\phi M_{B_s}^{3/2} m_b \alpha_1 \mu_{eff}}{3 m_\phi} (C_7 C_9 x_{B_s^*} - 2 C_7^2 x_b)\right] \frac{(1-s)^3}{s - x_{B_s^*}^2},
\end{aligned} \tag{3.23}$$

where we have defined $X_{CKM} = (G_F^2 |V_{tb} V_{ts}^*|^2 M_{B_s}^2 \alpha_{EM}^3)/(768\pi^4)$, $x_b \equiv m_b/M_{B_s}$, and $x_{B_s^*} \equiv M_{B_s^*}/M_{B_s}$. We use the Wilson coefficients $C_i(\lambda)$ choosing the scale at $\lambda \simeq m_b \simeq 5GeV$, with $C_7 = 0.312$, $C_9 = -4.21$ and $C_{10} = 4.64$ [43][58]. The CKM matrix elements are $|V_{tb} V_{ts}^*| = (4.7 \pm 0.8) \times 10^{-2}$ [59]. With the most recent lattice calculation of f_{B_s} is ≈ 228 MeV [60]. Note that, when integrated over the endpoint window the last two terms in Eq. (3.22) are much smaller than the first one. The interference contribution is destructive

and is

$$\mathcal{B}(B_s \to \mu^+\mu^-\gamma_{E<60})_{\phi B_s^*} = -5.0 \times 10^{-17}, \tag{3.24}$$

$$\mathcal{B}(B_s \to \mu^+\mu^-\gamma_{E<300})_{\phi B_s^*} = -1.1 \times 10^{-14}, \tag{3.25}$$

which are both much smaller than the B_s^* contribution alone.

The normalized differential spectrum in s is shown in Fig.(3.2.3). The photon energy is related to the invariant mass as $E_\gamma = (1-s)M_B/2$, so we can integrate the differential spectrum over the required corresponding kinematic region in photon energy to obtain the decay width.

Integrating Eq.(3.22) over the kinematic region corresponding to a soft photon cut of $E_\gamma \sim 60, 300$ MeV we get the respective branching ratios

$$\mathcal{B}(B_s \to \mu^+\mu^-\gamma_{E<60}) = 1.6 \times 10^{-12}, \tag{3.26}$$

$$\mathcal{B}(B_s \to \mu^+\mu^-\gamma_{E<300}) = 1.1 \times 10^{-10}, \tag{3.27}$$

which are quite too low to affect experimental determination of the branching ratio $B_s \to \mu^+\mu^-$, agreeing with the estimates of Ref. [40] where $\mathcal{B}_{\mathcal{SM}}(B_s^0 \to \mu^+\mu^-) = (3.23 \pm 0.27) \times 10^{-9}$.

3.3 $B_s^0 \to \mu^+\mu^-\nu_\mu\bar{\nu}_\mu$ transition

Because of the Glashow-Illiopulous-Maiani (GIM) mechanism, the SM loop diagram for the helicity-suppressed $B_s^0 \to \mu^+\mu^-$ decay is dominated by the intermediate top quark despite being suppressed by the CKM factors $|V_{tb}V_{ts}^*|^2$. A transition similar to the ones described above, which on a portion of the available phase space looks like $B_s^0 \to \mu^+\mu^-$ is the tree-level decay $B_s^0 \to \mu^+\mu^-\nu\bar{\nu}$. The dominant tree-level contribution for this process is depicted in

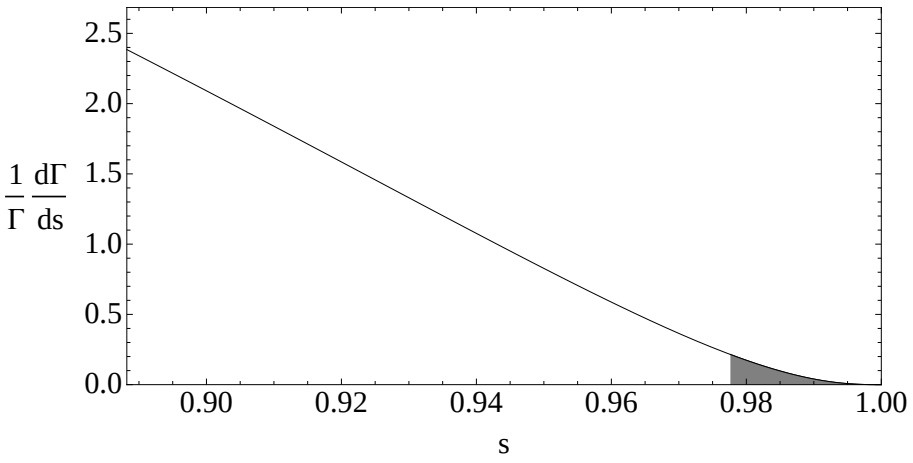

Figure 3.2.3: Normalized differential spectrum in s. The grey shaded region corresponds to the contribution from a soft photon energy cut at $E_\gamma \sim 60$ MeV.

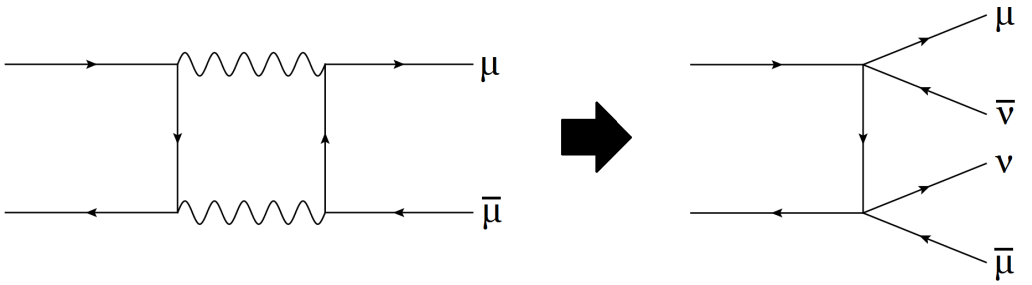

Figure 3.3.1: $B_s \to \mu^+\mu^-\bar{\nu}\nu$

Fig. 3.3.1. This decay can have a contribution to the background, which appears only below $q^2 = M_{B_s}^2$ and, if numerically significant, can affect the extraction of $\mathcal{B}(B_s \to \mu^+\mu^-)$. This process is neither loop-dominated nor is it helicity suppressed. It nevertheless has a kinematic phase space suppression due to the four-particle final state. For the B_s meson decay, an intermediate charm quark will give the largest contribution since the intermediate top quark diagram will be suppressed by the mass of the top quark. Also, the up quark contribution is suppressed by $V_{ub}V_{us}^* \approx \lambda^4$ whereas the charm contribution is only suppressed by $V_{cb}V_{cs}^* \approx \lambda^2$, where $\lambda \approx 0.22$.

The transition amplitude for this process is simple,

$$\mathcal{M}_{B_s\to\mu^+\mu^-\nu\bar{\nu}} = \frac{G_F^2}{2} V_{cb}V_{cs}^* \langle 0|\bar{s}\gamma_\beta(1-\gamma_5)\frac{i(\not{p}_c + m_c)}{p_c^2 - m_c^2}\gamma_\alpha(1-\gamma_5)b|B_s\rangle L_1^\alpha L_2^\beta, \tag{3.28}$$

where $L^\alpha = \bar{\mu}\gamma^\alpha(1-\gamma_5)\nu_\mu$. In the rest frame of the decaying meson we can reduce the phase space integral's dependence to five independent Lorentz invariants. In the same fashion as in [61] we define these invariants as

$$\begin{aligned} S_{12} = (p_{\mu^-} + p_{\mu^+})^2, \quad S_{13} &= (p_{\mu^-} + p_{\bar{\nu}})^2, \quad S_{34} = (p_{\bar{\nu}} + p_\nu)^2, \\ S_{123} = (p_{\mu^-} + p_{\mu^+} + p_{\bar{\nu}})^2 \quad &, \qquad S_{134} = (p_{\mu^-} + p_{\bar{\nu}} + p_\nu)^2. \end{aligned} \tag{3.29}$$

Our width then becomes

$$d\Gamma = \frac{(2\pi)^4}{2M}\int\left(\frac{\pi^2}{2M^2}\right)\frac{|\mathcal{M}_{B_s\to\mu^+\mu^-\nu\bar{\nu}}|^2}{[-\Delta_4(p_{\mu^-}, p_{\mu^+}, p_{\bar{\nu}}, p_\nu)]^{1/2}} dS_{12}dS_{123}dS_{13}dS_{134}, \tag{3.30}$$

where Δ_4 is the symmetric Gram determinant

$$\Delta_4(q,r,s,t) = \begin{vmatrix} q^2 & q\cdot r & q\cdot s & q\cdot t \\ r\cdot q & r^2 & r\cdot s & r\cdot t \\ s\cdot q & s\cdot r & s^2 & s\cdot t \\ t\cdot q & t\cdot r & t\cdot s & t^2 \end{vmatrix}. \tag{3.31}$$

In order to avoid the divergence of $1/(-\Delta_4)^{1/2}$ on the boundary, suitable variable changes can be made thereby making the singularity integrable. We define

$$\begin{aligned} S_{134} &= \frac{1}{2a}\left[-b + \sin(\tilde{S}_{134})(b^2 - 4ac)^{1/2}\right], \\ S_{13} &= 4(-a)^{1/2}\tilde{S}_{13} + m_\ell^2, \end{aligned} \tag{3.32}$$

where a, b and c are the parameters solved by

$$-\Delta_4(p_{\mu^-}, p_{\mu^+}, p_{\bar{\nu}}, p_\nu) = aS_{134}^2 + bS_{134} + c\,. \tag{3.33}$$

The limits of integration are calculated in [61], resulting in our partial width

$$\frac{d\Gamma}{dS_{12}} = \frac{2}{(4\pi)^6 M^3} \int_{S_{12}}^{M^2} dS_{123} \int_0^{\xi} dS_{34} \int_{m_\ell^2/S_{12}}^{1} d\tilde{S}_{13} \int_{-\pi/2}^{\pi/2} d\tilde{S}_{134} \left|\mathcal{M}_{B_s\to\mu^+\mu^-\nu\bar{\nu}}\right|^2, \tag{3.34}$$

where $\xi = (M^2 - S_{123})(S_{123} - S_{12})/S_{123}$. We define the cut on missing energy as $S_{12}^{cut}(E_{cut}) = M^2 - 2M(E_{cut})$ which gives us a lower limit on S_{12} for the final integral in order to obtain the decay width. The branching ratios for this contribution can then calculated using numerical phase-space integration for various cuts including the one that corresponds to the invariant mass range seen at the LHCb.

$$\begin{aligned} BR\left[B_s \to \mu^+\mu^-\nu\bar{\nu}\right]_{E_{cut}=60MeV} &= 1.6 \times 10^{-25} \\ BR\left[B_s \to \mu^+\mu^-\nu\bar{\nu}\right]_{E_{cut}=300MeV} &= 1.4 \times 10^{-18}. \end{aligned} \tag{3.35}$$

As we can see, the due to enormous phase space suppression (we are only interested in a small sliver of the available four-particle final state), the possible contribution from this decay is unimportant for experimental analyses.

3.4 Conclusion

We have seen from the above calculation that addition soft photon contributions can affect the experimental branching ratio of $B_s \to \mu^+\mu^-$ by 1 to 3 % depending on the energy resolution of the detector. While not helicity suppressed, the phase space is quite small and leads to a small contribution.

CHAPTER 4

SUPER-WIMPS AND $(B, D) \to \ell\bar{\nu}_\ell$

This work was published in [28].

4.1 Introduction

There is evidence that the amount of dark matter (DM) in the Universe by far dominates that of the luminous matter. It comes from a variety of cosmological sources such as the rotation curves of galaxies [13, 14, 15], gravitational lensing, features of CMB [16] and large scale structures [17]. While the presence of DM is firmly established, its basic properties are still subject of a debate. If dark matter is comprised from some fundamental particle, experimentally-measured properties, such as its relic abundance or production cross-sections can be predicted. Experimental measurements of the abundance $\Omega_{DM}h^2 \sim 0.12$ by WMAP collaboration [2] can be used to place constraints on the masses and interaction strengths of those DM particles. Indeed, the relation

$$\Omega_{DM}h^2 \sim \langle \sigma_{ann} v_{rel} \rangle^{-1} \propto \frac{M^2}{g^4}, \tag{4.1}$$

with M and g being the mass and the interaction strength associated with DM annihilation, implies that, for a weakly-interacting massive particle (WIMP) of DM, the mass scale should be set around the electroweak scale. Yet, difficulties in understanding of small-scale gravitational clustering in numerical simulations with WIMPs may lead to preference being given to much lighter DM particles. Particularly there has been interest in studying models of light dark matter particle with masses of the keV range [20, 21]. According to Eq. (4.1), the light mass of dark matter particle then implies a superweak interaction between the dark

matter and standard model (SM) sector [22, 23]. Several models with light $\mathcal{O}$(keV-MeV) DM particles, or super-WIMPs, have been proposed [20, 21].

One of the main features of the super-WIMP models is that DM particles do not need to be stable against decays to even lighter SM particles [20]. This implies that one does not need to impose an ad-hoc Z_2 symmetry when constructing an effective Lagrangian for DM interactions with the standard model fields, so DM particles can be emitted and absorbed by SM particles. Due to their extremely small couplings to the SM particles, experimental searches for super-WIMPs must be performed at experiments where large statistics is available. In addition, the experiments must be able to resolve signals with missing energy [24]. Super-B factories fit this bill perfectly.

In this paper we focus on bosonic super-WIMP models [20, 21] for dark matter candidates and attempt to constrain their couplings with the standard model through examining leptonic meson decays. The idea is quite straightforward. In the standard model the leptonic decay width of, say, a B-meson, i.e. the process $B \to \ell\bar{\nu}$, is helicity-suppressed by $(m_\ell/m_B)^2$ due to the left-handed nature of weak interactions [62],

$$\Gamma(B \to \ell\bar{\nu}) = \frac{G_F^2}{8\pi}|V_{ub}|^2 f_B^2 m_B^3 \frac{m_\ell^2}{m_B^2}\left(1 - \frac{m_\ell^2}{m_B^2}\right)^2. \tag{4.2}$$

Similar formula is available for charmed meson D^+ and D_s decays with obvious substitution of parameters. The only non-perturbative parameter affecting Eq. (4.2), the heavy meson decay constant f_B, can be reliably estimated on the lattice [63], so the branching ratio for this process can be predicted quite reliably.

The helicity suppression arises from the necessary helicity flip on the outgoing lepton due to angular momentum conservation as initial state meson is spinless. The suppression can be overcome by introducing a third particle to the final state that contributes to total angular momentum [45] (see Fig. 4.1.1). If that particle is a light DM candidate, helicity suppression is traded for a small coupling strength of DM-SM interaction. In this case, the

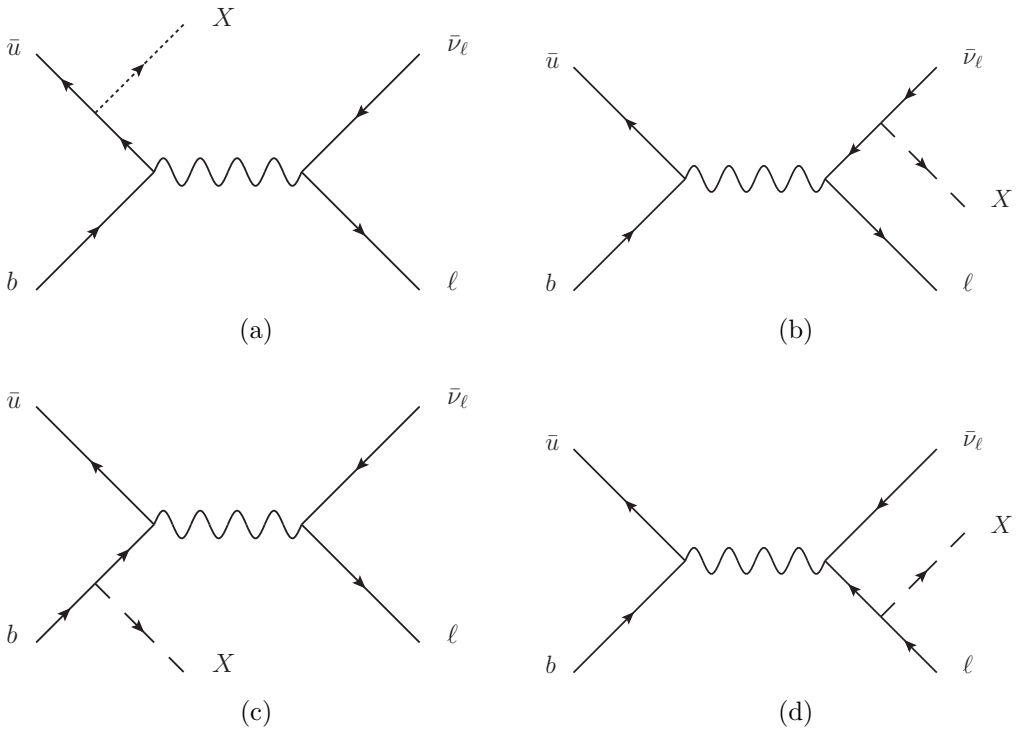

Figure 4.1.1: Diagrams for the super-WIMP emission in $B \to \ell\bar{\nu}_\ell X$. Similar diagrams exist for $D_{(s)}$ decays. Note that the graph (b) is absent for the vector light dark matter particles discussed in section 4.4.

charged lepton spectrum of the 3-body $B \to \ell\bar{\nu}_\ell + X$ (with X being the DM candidate) process will be markedly different from the spectrum of two-body $B \to \ell\bar{\nu}_\ell$ decay. Then, the rate for the process $B \to \ell + \not{E}$, with $\not{E}$ being missing energy, can be used to constrain properties of light DM particles.

We shall consider two examples of super-WIMPs, the "dark photon" spin-1 particle, and a spin-0, axion-like state. The discussion of the vector dark matter effects is similar to a calculation of the radiative leptonic decay [45], i.e. the spin of the added DM particle brings the needed unit of angular momentum. In the case of axion-like DM candidate, there is a derivative coupling to the SM allowing the pseudoscalar particle to carry orbital angular momentum and hence overcome helicity suppression as well. As a side note, we add that the models of new physics considered here are very different from the models that are usually constrained in the new physics searches with leptonic decays of heavy mesons [64, 65].

This paper is organized as follows. In Section 4.2 we examine the decay width for the process $M \to \ell\bar{\nu}_\ell + X$ for $X = a$ being a spin-0 particle. We consider a particular two-Higgs doublet model, taking into account DM-Higgs mixing in Section 4.3. In Section 4.4 we consider constraints on a spin-1 super-WIMP candidate. We conclude in Section 4.5.

4.2 Simple Axion-Like Dark Matter

We consider first an "axion-like" dark matter (ALDM) model, as suggested in [20] and study the tree-level interactions with the standard model fermions. The most general Lagrangian consists of a combination of dimension-five operators,

$$\mathcal{L}_a = -\frac{\partial_\mu a}{f_a}\bar{\psi}\gamma^\mu\gamma_5\psi + \frac{C_\gamma}{f_a}aF_{\mu\nu}\widetilde{F}^{\mu\nu}, \tag{4.3}$$

where $X = a$ is the DM particle and the coupling constant f_a has units of mass. Taking into account the chiral anomaly we can substitute the second term with a combination of vector

and axial-vector fermionic currents,

$$\mathcal{L}_a = -\left(\frac{1}{f_a} + \frac{4\pi C_\gamma}{f_a \alpha}\right)\partial_\mu a \; \bar{\psi}\gamma^\mu\gamma_5\psi - im_\psi\left(\frac{8\pi C_\gamma}{f_a\alpha}\right)a\bar{\psi}\gamma_5\psi. \tag{4.4}$$

The feynman diagrams that contribute to the meson decay, for example $B \to \ell\bar{\nu}_\ell + a$, are shown by Fig 4.1.1. The amplitude for the emission of a in the transition $M \to \ell\bar{\nu}_\ell + a$ can be written as

$$\mathcal{A}_{M\to\ell\bar{\nu}a} = \mathcal{A}_\ell + \mathcal{A}_q, \tag{4.5}$$

where $\mathcal{A}_q$, the quark contribution, represents emission of a from the quarks that build up the meson and $\mathcal{A}_\ell$, the leptonic contribution, describe emission of a from the final state leptons.

Let's consider the lepton amplitude first. Here we can parameterize the axial matrix elements contained in the amplitude in terms of the decay constant f_B such as

$$\langle 0|\bar{u}\gamma^\mu\gamma_5 b|B\rangle = if_B P_B^\mu, \tag{4.6}$$

If the mass of the axion-like DM particle is small ($m_a \to 0$), the leptonic contribution simplifies to

$$\mathcal{A}_\ell = i\sqrt{2}G_F V_{ub}\frac{f_M}{f_a}m_\ell\left(\frac{m_\ell}{2k\cdot p_\ell}[\bar{u}_\ell \; \not{k}(1-\gamma_5)v_\nu] - [\bar{u}_\ell(1-\gamma_5)v_\nu]\right). \tag{4.7}$$

Here k is the DM momentum. Clearly, this contribution is proportional to the lepton mass and can, in principle, be neglected in what follows. The contribution to the decay amplitude from the DM emission from the quark current is

$$\mathcal{A}_q = i\langle 0|\bar{u}\Gamma^\mu b|B\rangle[\bar{u}_\ell\gamma_\mu(1-\gamma_5)v_\nu] \tag{4.8}$$

where the current $\bar{u}\Gamma^{\mu}b$ is obtained from the diagrams in Figure 4.1.1 (a) and (c),

$$\Gamma^{\mu} = \frac{G_F}{\sqrt{2}f_a}V_{ub}\left[\frac{(\not{k}\gamma_5)(\not{k}-\not{p}_u+m_u)\gamma^{\mu}(1-\gamma_5)}{m_a^2-2p_u\cdot k}+\frac{\gamma^{\mu}(1-\gamma_5)(\not{p}_b-\not{k}+m_b)(\not{k}\gamma_5)}{m_a^2-2p_b\cdot k}\right]. \quad (4.9)$$

Since the meson is a bound state of quarks we must use a model to describe the effective quark-antiquark distribution. We chose to follow Refs. [66] and [67], where the wave function for a ground state meson M can be written in the form

$$\psi_M = \frac{I_c}{\sqrt{6}}\phi_M(x)\gamma_5(\not{P}_M + M_M g_M(x)). \quad (4.10)$$

Here I_c is the identity in color space and x is the momentum fraction carried by one of the quarks. For a heavy meson H it would be convenient to assign x as a momentum fraction carried by the heavy quark. Also, for a heavy meson, $g_H \sim 1$, and in the case of a light meson $g_L = 0$. For the distribution amplitudes of a heavy or light meson we use

$$\phi_L \sim x(1-x), \quad (4.11)$$

$$\phi_H \sim \left[\frac{(m^2/M_H^2)}{1-x}+\frac{1}{x}-1\right]^{-2}, \quad (4.12)$$

where m is the mass of the light quark and the meson decay constant is related to the normalization of the distribution amplitude,

$$\int_0^1 \phi_M(x)dx = \frac{f_M}{2\sqrt{6}}. \quad (4.13)$$

The matrix element can then be calculated by integrating over the momentum fraction [67]

$$\langle 0|J^{\mu}|M\rangle = \int_0^1 dx\ \mathrm{Tr}\left[\Gamma^{\mu}\psi_M\right]. \quad (4.14)$$

Neglecting the mass of the axion-like DM particle, the decay amplitude simplifies to

$$\mathcal{A}_q = i\frac{\sqrt{3}G_F V_{ub} M_B}{f_a(k\cdot P_B)}\left(M_B\Phi_1^B - m_b\Phi_0^B\right)\left[\bar{\ell}\ \not{k}(1-\gamma_5)\nu\right], \tag{4.15}$$

where m_b is the mass of the b-quark (or, in general, a down-type quark in the decay), and we defined

$$\Phi_n^M = \int_0^1 \frac{\phi_M(x)}{x(1-x)}x^n dx \tag{4.16}$$

The total decay width is, then,

$$\begin{aligned}\Gamma_{B\to a\ell\nu_\ell} &= \frac{G_F^2 f_B^2 |V_{ub}|^2 M_B^5}{64\pi^3 f_a^2}\left[\frac{1}{6}(2\rho^2+3\rho^4+12\rho^4\log\rho-6\rho^6+\rho^8)\right.\\ &+ \left. g_B^2\ \Phi(m_b,M_B)^2(1-6\rho^2-12\rho^4\log\rho+3\rho^4+2\rho^6)\right],\end{aligned} \tag{4.17}$$

where $\rho \equiv m_\ell/m_B$. Also,

$$\Phi(m_b,M_B) = \frac{m_b\Phi_0 - M_B\Phi_1}{f_B M_B}. \tag{4.18}$$

Note that $\Phi(m_b,M_B) \propto 1/m$, which is consistent with spin-flipping transition in a quark model, which would explain why this part of the decay rate is not proportional to m_ℓ. Similar results for other heavy mesons, like D^+ and D_s^+ are obtained by the obvious substitution of relevant parameters, such as masses, decay constants and CKM matrix elements.

Experimentally, the leptonic decays of heavy mesons are best studied at the e^+e^- flavor factories where a pair of M^+M^- heavy mesons are created. The study is usually done by fully reconstructing one of the heavy mesons and then by finding a candidate lepton track of opposite sign to the tagged meson. The kinematical constraints on the lepton are then used to identify the decays with missing energy as leptonic decay.

In the future super-B factories, special studies of the lepton spectrum in $M \to \ell$+missing energy can be done using this technique to constrain the DM parameters from Eq. (4.17). The lepton energy distributions, which are expected to quite different for the three-body

decays $B^- \to a\ell^-\bar{\nu}_\ell$ are shown (normalized) in Fig. 4.2.1 for each lepton decay process. However, we can put some constraints on the DM coupling parameters using the currently available data on $M \to \ell\bar{\nu}_\ell$. The experimental procedure outlined above implies that what is experimentally detected is the combination,

$$\begin{aligned}\Gamma_{\rm exp}(M \to \ell\bar{\nu}_\ell) &= \Gamma_{\rm SM}(M \to \ell\bar{\nu}_\ell) + \int_{E<E_0} dE_a \frac{d\Gamma(M \to a\ell\bar{\nu}_\ell)}{dE_a} \\ &= \Gamma_{\rm SM}(M \to \ell\bar{\nu}_\ell)\ [1 + R_a(E_0)]\,, \end{aligned} \tag{4.19}$$

where E_0 is the energy cutoff that is specific for each experiment. Equivalently, cutoff in q^2 can also be used. In the above formula we defined

$$R_a(E_0) = \frac{1}{\Gamma_{\rm SM}(M \to \ell\bar{\nu}_\ell)} \int_{E<E_0} dE_a \frac{d\Gamma(M \to a\ell\bar{\nu}_\ell)}{dE_a}. \tag{4.20}$$

Our bounds on the DM couplings from different decay modes are reported in Table 7.0.1 in the appendix for the cutoff values of $E_0 = 100$ MeV. Note that similar expressions for the leptonic decays of the *light* mesons, such as $\pi \to a\ell\bar{\nu}$ and $K \to a\ell\bar{\nu}$ come out to be proportional to the mass of the final state lepton. This is due to the fact that in the light meson decay the term proportional to g vanishes. Thus, those decays do not offer the same relative enhancement of the three-body decays due to removal of the helicity suppression in the two-body channel. It is interesting to note that the same is also true for the heavy mesons if a naive Non-Relativistic Constituent Quark Model (NRCQM), similar to the one used in Refs. [68, 69] is employed. We checked that a simple replacement

$$p_b = \frac{m_b}{m_B} P_B, \qquad\qquad p_u = \frac{m_u}{m_B} P_B \tag{4.21}$$

advocated in [68, 69] is equivalent to use of symmetric (with respect to the momentum fraction carried by the heavy quark) distribution amplitude, which is not true in general.

Currently, the SM predictions for the $B^- \to \ell^- \bar{\nu}_\ell$ decay for $\ell = \mu, e$ are significantly smaller than the available experimental upper bounds [70, 71], which is due to the smallness of V_{ub} and the helicity suppression of this process. This, even in the standard model, there is a possibility that some of the processes $B^- \to \gamma_s \ell^- \bar{\nu}_\ell$, with γ_s being the soft photon missed by the experimental detector. Such photons would affect the bounds on the DM couplings reported in Table 7.0.1.

The issue of the soft photon "contamination" of $B^- \to \ell^- \bar{\nu}_\ell$ is non-trivial if model-independent estimates of the contributions are required (for the most recent studies, see [44]). In order to take those into account, the formal in Eq. (4.19) should be modified to

$$\Gamma_{\rm exp}(M \to \ell \bar{\nu}_\ell) \;=\; \Gamma_{\rm SM}(M \to \ell \bar{\nu}_\ell) \;\left[1 + R_a(E_0) + R_{\gamma_s}(E_0')\right]. \tag{4.22}$$

In general, the experimental soft photon cutoff E_0' could be different from the DM emission cutoff E_0. Since we are only interested in the upper bounds on the DM couplings, this issue is not very relevant here, as the amplitudes with soft photons do not interfere with the amplitudes with DM emission. Nevertheless, for the purpose of completeness, we evaluated the possible impact of undetected soft photons using NRCQM as seen in [68, 69]. The results are presented in Table 7.0.1 in the appendix of this dissertation for different values of cutoff on the photon's energy. We present the NRCQM mass parameters in Table 4.2.1 with the decay constants calculated in [72].

The relevant plots for D (D_s) decays can be obtained upon substitution $M_B \to M_{D(D_s)}$, $f_B \to f_{D(D_s)}$, and $V_{ub} \to V_{cd(cs)}$. Note that there is no CKM suppression for D_s decays. In order to bound f_a we use the experimentally seen transitions $B \to \tau\bar{\nu}$, $D_{(s)} \to \mu\bar{\nu}$, and $D_s \to \tau\bar{\nu}$. We note that the soft photon "contamination" can be quite large, up to 10% of the standard model prediction for the two body decay.

The resulting fits on f_a can be found in Table 4.2.2. As one can see, the best constraint comes from the $D^\pm \to \mu^\pm \bar{\nu}_\mu$ decay where experimental and theoretical branching ratios are

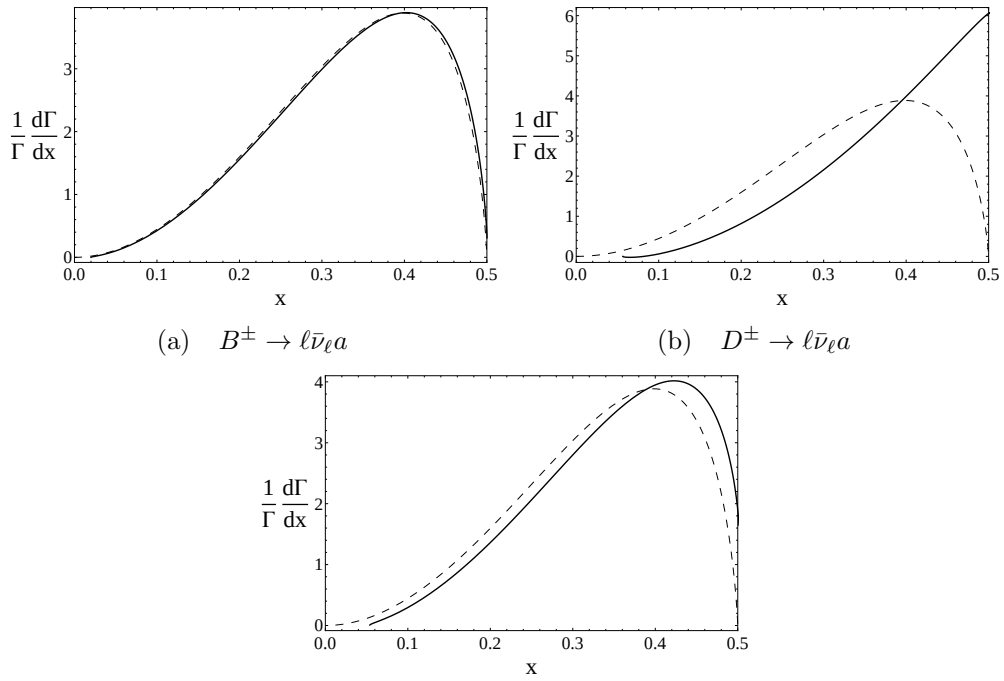

(a) $B^{\pm} \to \ell \bar{\nu}_{\ell} a$ (b) $D^{\pm} \to \ell \bar{\nu}_{\ell} a$

(c) $D_s^{\pm} \to \ell \bar{\nu}_{\ell} a$

Figure 4.2.1: Normalized electron (solid) and muon (dashed) energy distributions for the heavy $(B^{\pm}, D^{\pm}, D_s^{\pm})$ meson decay channels.

in close agreement.

4.3 Axion-like Dark Matter in a Type II Two Higgs Doublet Model

A generic axion-like DM considered in the previous section was an example of a simple augmentation of the standard model by an axion-like dark matter particle. A somewhat different picture can emerge if those particles are embedded in more elaborate beyond the standard model (BSM) scenarios. For example, in models of heavy dark matter of the "axion portal"-type [74], spontaneous breaking of the Peccei-Quinn (PQ) symmetry leads to an axion-like particle that can mix with the CP-odd Higgs A^0 of a two Higgs Doublet model (2HDM). For the sufficiently small values of its mass this state itself can play a role of the light

Quark	Constituent Mass
m_u	335.5 MeV
m_d	339.5 MeV
m_s	486 MeV
m_c	1550 MeV
m_b	4730 MeV

Table 4.2.1: Constituent quark masses [73] used in calculations.

Channel	f_a, MeV
$\mathcal{B}\left(B^{\pm} \to \tau^{\pm}\bar{\nu}_{\tau}\right)$	12
$\mathcal{B}\left(D^{\pm} \to \mu^{\pm}\bar{\nu}_{\mu}\right)$	236
$\mathcal{B}\left(D_s^{\pm} \to \mu^{\pm}\bar{\nu}_{\mu}\right)$	62
$\mathcal{B}\left(D_s^{\pm} \to \tau^{\pm}\bar{\nu}_{\tau}\right)$	11

Table 4.2.2: Constraint on f_a using the various seen decay channels.

DM particle. The decays under consideration can be derived from the $B \to \ell\nu A^0$ amplitude. An interesting feature of this model is the dependence of the light DM coupling upon the quark mass. This means that the decay rate would be dominated by the contributions enhanced by the heavy quark mass. This would also mean that the astrophysical constraints on the axion-like DM parameters might not probe all of the parameter space if this model.

In a concrete model [74], the PQ symmetry $U(1)_{PQ}$ is broken by a large vacuum expectation value $\langle S\rangle \equiv f_a \gg v_{EW}$ of a complex scalar singlet Φ. As in [75], we shall work in an interaction basis so that the axion state appears in Φ as

$$\Phi = f_a \exp\left[\frac{ia}{\sqrt{2}f_a}\right] \tag{4.23}$$

and A^0 appears in the Higgs doublets in the form

$$\Phi_u = \begin{pmatrix} v_u \exp\left[\frac{i\cot\beta}{\sqrt{2}v_{EW}}A^0\right] \\ 0 \end{pmatrix}, \qquad \Phi_d = \begin{pmatrix} 0 \\ v_d \exp\left[\frac{i\tan\beta}{\sqrt{2}v_{EW}}A^0\right] \end{pmatrix}, \tag{4.24}$$

where we suppress the charged and CP-even Higgses for simplicity and define $\tan\beta = v_u/v_d$ and $v_{EW} = \sqrt{v_u^2 + v_d^2} \equiv \frac{m_W}{g}$. We choose the operator that communicates PQ charge to the standard model to be of the form[1]

$$\mathcal{L} = \lambda \Phi^2 \Phi_u \Phi_d + h.c. \tag{4.25}$$

This term contains the mass terms and, upon diagonalizing, the physical states in this basis are given by [75]

$$a_p = a\cos\theta - A^0 \sin\theta \tag{4.26}$$

$$A_p^0 = a\sin\theta + A^0\cos\theta \tag{4.27}$$

where $\tan\theta = (v_{EW}/f_a)\sin 2\beta$. Here a_p denotes the "physical" axion-like state. Thus, the amplitude for $B \to \ell\nu a_p$ can be derived from

$$\mathcal{M}(B \to \ell\nu a_p) = -\sin\theta \mathcal{M}(B \to \ell\nu A^0) + \cos\theta\ \mathcal{M}(B \to \ell\nu a) \tag{4.28}$$

In a type II 2HDM [75, 76, 77], the relevant Yukawa interactions of the CP-odd Higgs with fermions are given by

$$\mathcal{L}_{A^0 f\bar{f}} = \frac{ig\tan\beta}{2m_W} m_d \bar{d}\gamma_5 d A^0 + \frac{ig\cot\beta}{2m_W} m_u \bar{u}\gamma_5 u A^0 \tag{4.29}$$

where $d = \{d, s, b\}$ refers to the down type quarks and $u = \{u, c, t\}$ refers to the up type quarks. The interaction with leptons are the same as above with $d \to \ell$ and $u \to \nu$.

In the axion portal scenario the axion mass is predicted to lie within a specific range of $360 < m_a \leq 800$ MeV to explain the galactic positron excess [74]. Using the quark model

[1] This is the case of the so-called Dine-Fischler-Srednicki-Zhitnitsky (DFSZ) axion, although other forms of the interaction term with other powers of the scalar field Φ are possible [75].

introduced in the previous section we obtain the decay width

$$\begin{aligned}\Gamma\left(B\to\ell\nu_\ell a_p\right) &= \frac{G_F^2|V_{ub}|^2 m_B^3}{256\pi^3\left(f_a^2+v_{EW}^2\sin^2 2\beta\right)}\\ &\times\left[\cos 2\beta\left(m_u\Phi_1^B+m_b(\Phi_0^B-\Phi_1^B)\right)+5\left[m_b(\Phi_1^B-\Phi_0^B)+m_u\Phi_1^B\right]\right]^2\\ &\times\left[12x_a^4\log(x_a)-4x_a^6+3x_a^4+(\rho-1)^4(4(\rho-2)\rho+1)-12(\rho-1)^4\log(1-\rho)\right]\end{aligned} \tag{4.30}$$

Here we defined $x_a = m_a/m_B$, and $\rho = m_\ell/m_B$. If we assume $f_a \gg v_{EW}\sin 2\beta$ we can then provide bounds on f_a as seen in Table 4.3.1. Just like in the previous section, the results for

	$f_a(MeV)$	$f_a(MeV)$	$f_a(MeV)$	$f_a(MeV)$
Channel	$\tan\beta=1$	$\tan\beta=5$	$\tan\beta=10$	$\tan\beta=20$
$\mathcal{B}\left(B^\pm\to\tau^\pm\bar{\nu}_\tau\right)$	70	340	357	361
$\mathcal{B}\left(D^\pm\to\mu^\pm\bar{\nu}_\mu\right)$	416	2874	3078	3131
$\mathcal{B}\left(D_s^\pm\to\mu^\pm\bar{\nu}_\mu\right)$	532	1380	1499	1529

Table 4.3.1: Constraint on f_a using the observed decays for various $\tan\beta$s.

other decays, such as $D_{(s)}\to\ell\bar{\nu}_\ell$, can be obtained by the trivial substitution of masses and decay constants.

4.4 Light Vector Dark Matter

Another possibility for a super-WIMP particle is a light (keV-range) vector dark matter boson (LVDM) coupled to the SM solely through kinetic mixing with the hypercharge field strength [20]. This can be done consistently by postulating an additional $U(1)_V$ symmetry. The relevant terms in the Lagrangian are

$$\mathcal{L} = -\frac{1}{4}F_{\mu\nu}F^{\mu\nu}-\frac{1}{4}V_{\mu\nu}V^{\mu\nu}-\frac{\kappa}{2}V_{\mu\nu}F^{\mu\nu}+\frac{m_V^2}{2}V_\mu V^\mu+\mathcal{L}_{h'}, \tag{4.31}$$

where $\mathcal{L}_{h'}$ contains terms with, say, the Higgs field which breaks the $U(1)_V$ symmetry, κ parameterizes the strength of kinetic mixing, and, for simplicity, we directly work with the photon field A_μ. In this Lagrangian only the photon A_μ fields (conventionally) couple to the SM fermion currents.

It is convenient to rotate out the kinetic mixing term in Eq. (4.31) with field redefinitions

$$A \to A' - \frac{\kappa}{\sqrt{1-\kappa^2}} V', \qquad\qquad V \to \frac{1}{\sqrt{1-\kappa^2}} V'. \tag{4.32}$$

The mass m_V will now be redefined as $m_V \to \frac{m_V}{\sqrt{1-\kappa^2}}$. Also, both A'_μ and V'_μ now couple to the SM fermion currents via

$$\mathcal{L}_f = -eQ_f A'_\mu \bar{\psi}_f \gamma^\mu \psi_f - \frac{\kappa e Q_f}{\sqrt{1-\kappa^2}} V'_\mu \bar{\psi}_f \gamma^\mu \psi_f, \tag{4.33}$$

where Q_f is the charge of the interacting fermion thus introducing our new vector boson's coupling to the SM fermions. Calculations can be now carried out with the approximate modified charge coupling for $\kappa \ll 1$,

$$\frac{\kappa e}{\sqrt{1-\kappa^2}} \approx \kappa e. \tag{4.34}$$

As we can see, in this case the coupling of the physical photon did not change much compared to the original field A_μ, while the DM field V'_μ acquired small gauge coupling κe. It is now trivial to calculate the process $B \to \ell \bar{\nu} V_{DM}$, as it can be done similarly to the case of the soft photon emission in Sect. 4.2. Employing the gauge condition $\epsilon \cdot k = 0$ for the DM fields, the amplitudes become in the limit $m_V \to 0$

$$\mathcal{A}_q = i \frac{G_F V_{ub} \kappa e \epsilon^{*\alpha}}{6k \cdot p_B} \left[A^\mu_\alpha \bar{\ell} \gamma_\mu (1-\gamma_5) \nu_\ell + B \bar{\ell} \gamma_\alpha (1-\gamma_5) \nu_\ell + C_\alpha \bar{\ell} (1-\gamma_5) \nu_\ell, + D^\mu \bar{\ell} \sigma_{\mu\alpha} (1+\gamma_5) \nu_\ell \right] \tag{4.35}$$

with the coefficients

$$\begin{aligned}
A^{\mu}_{\alpha} &= \left[3\sqrt{2}f_B - 2\sqrt{3}(\Phi_0^B + \Phi_1^B)\right] k^{\mu}q^{\alpha} - 2\sqrt{3}(\Phi_0^B - 3\Phi_1^B)i\epsilon^{\mu\alpha\sigma\rho}k_{\sigma}q_{\rho}, \\
B &= -\left[3\sqrt{2}f_B - 2\sqrt{3}(\Phi_0^B + \Phi_1^B)\right](k\cdot q) - \frac{3}{\sqrt{2}}f_B m_B^2 \\
&\quad - 2\sqrt{3}gm_B\left[m_2(\phi_0 - 3\phi_1) + 2m_B\phi_1\right], \qquad (4.36) \\
C_{\alpha} &= 3\sqrt{2}f_B m_{\ell}\frac{q^{\alpha}k\cdot p_{\ell} - p_{\ell}^{\alpha}k\cdot q}{k\cdot p_{\ell}}, \\
D^{\mu} &= -3\sqrt{2}if_B m_{\ell}\frac{k\cdot q}{k\cdot p_{\ell}}k^{\mu},
\end{aligned}$$

and $q = p_{\ell} + p_{\nu}$. Again, we fit the parameter κ using the same data as in the axion-like DM

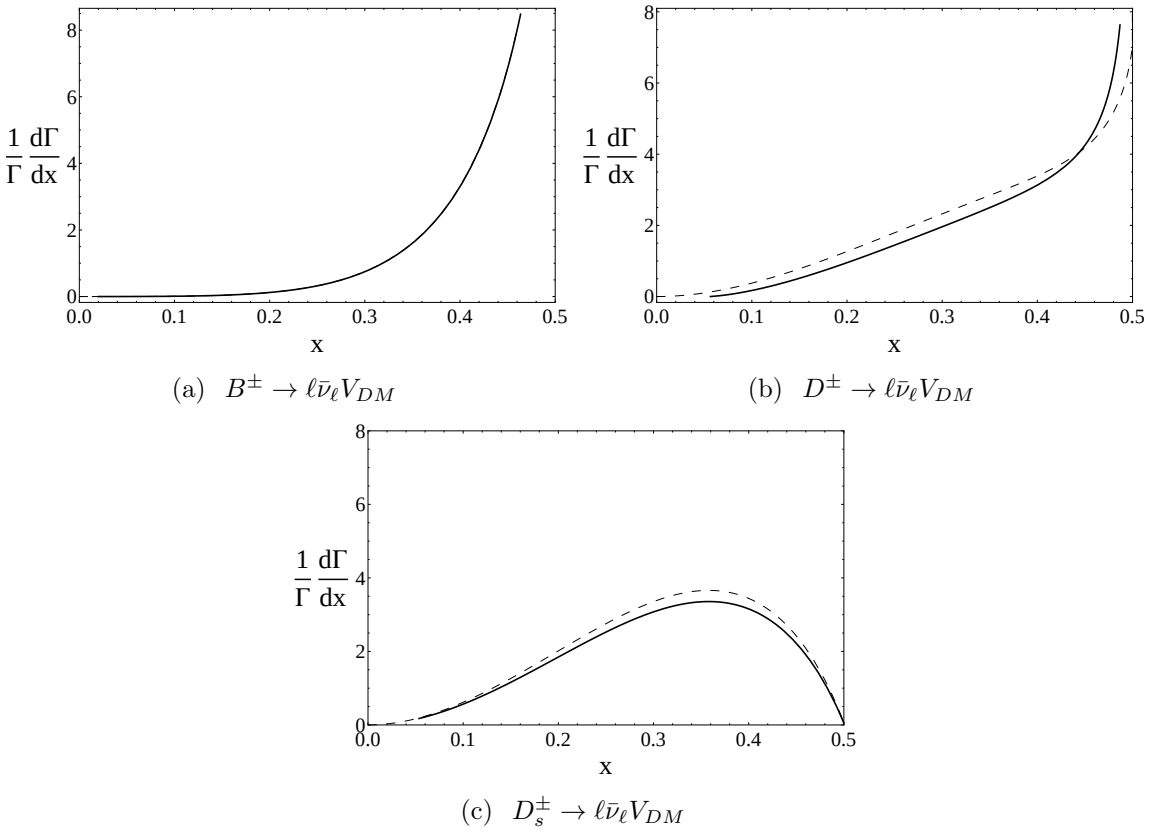

(a) $B^{\pm} \to \ell\bar{\nu}_{\ell}V_{DM}$ (b) $D^{\pm} \to \ell\bar{\nu}_{\ell}V_{DM}$

(c) $D_s^{\pm} \to \ell\bar{\nu}_{\ell}V_{DM}$

Figure 4.4.1: Normalized electron (dashed) and muon (solid) energy distributions for the heavy $\{(B^{\pm}, D^{\pm}, D_s^{\pm}\}$ meson decay channels.

case. The results are shown in Figure 4.4.1 where the $D^{\pm} \to \mu^{\pm}\bar{\nu}_{\mu}V$ decay can yield the

best bound. Using the best constraint on κ from the $D^{\pm} \to \mu^{\pm}\bar{\nu}_{\mu}V$ decay we can limit the

Channel	$\kappa^{-2}R_V(E_0)$ $E_0 = 100$ MeV	κ
$\mathcal{B}(B^{\pm} \to \tau^{\pm}\bar{\nu}_{\tau})$	8.8×10^{-3}	≤ 11.6
$\mathcal{B}(D^{\pm} \to \mu^{\pm}\bar{\nu}_{\mu})$	5.7×10^{-1}	≤ 0.31
$\mathcal{B}(D_s^{\pm} \to \mu^{\pm}\bar{\nu}_{\mu})$	5.4×10^{-2}	≤ 1.49
$\mathcal{B}(D_s^{\pm} \to \tau^{\pm}\bar{\nu}_{\tau})$	1.3×10^{-4}	≤ 20.8
$\mathcal{B}(B^{\pm} \to e^{\pm}\bar{\nu}_{e})$	1.8×10^{3}	≤ 11.2
$\mathcal{B}(B^{\pm} \to \mu^{\pm}\bar{\nu}_{\mu})$	1.0×10^{-1}	≤ 4.17
$\mathcal{B}(D^{\pm} \to e^{\pm}\bar{\nu}_{e})$	1.5×10^{3}	≤ 0.83
$\mathcal{B}(D^{\pm} \to \tau^{\pm}\bar{\nu}_{\tau})$	1.8×10^{-4}	≤ 36.4
$\mathcal{B}(D_s^{\pm} \to e^{\pm}\bar{\nu}_{e})$	5.2×10^{2}	≤ 1.37

Table 4.4.1: Constraints on κ using various decay channels. All other values are the same as in appendix Table 6.0.1.

contribution to yet-to-be-seen decays in Table 4.4.2.

As we can see, the constraints on the kinetic mixing parameter κ are not very strong, but could be improved in the next round of experiments at super-flavor factories.

4.5 Conclusions

We considered constraints on the parameters of different types of bosonic super-WIMP dark matter from leptonic decays of heavy mesons. The main idea rests with the fact that in the standard model the two-body leptonic decay width of a heavy meson $M = \{B, D_{(s)}\}$, or $\Gamma(M \to \ell\bar{\nu})$, is helicity-suppressed by $(m_{\ell}/m_B)^2$ due to the left-handed nature of weak interactions [62]. A similar three-body decay $M \to \ell\bar{\nu}_{\ell}X$ decay, which has similar

Channel	$\mathcal{B}(\kappa = 0.31)$
$\mathcal{B}(B^{\pm} \to e^{\pm}\bar{\nu}_{e})$	1.4×10^{-9}
$\mathcal{B}(B^{\pm} \to \mu^{\pm}\bar{\nu}_{\mu})$	3.6×10^{-9}
$\mathcal{B}(D^{\pm} \to e^{\pm}\bar{\nu}_{e})$	1.2×10^{-6}
$\mathcal{B}(D^{\pm} \to \tau^{\pm}\bar{\nu}_{\tau})$	1.7×10^{-8}
$\mathcal{B}(D_s^{\pm} \to e^{\pm}\bar{\nu}_{e})$	6.2×10^{-6}

Table 4.4.2: Contributions to various yet-to-be-seen channels using the the fit on κ in Table 4.4.1.

experimental signature, is not helicity suppressed. We put constraints on the couplings of such DM particles to quarks. We note that the models of new physics considered here are very different from the models that are usually constrained in the new physics searches with leptonic decays of heavy mesons [64].

CHAPTER 5

NEW PLAYERS IN RARE CHARM DECAYS

5.1 Introduction

Flavor changing neutral currents are allowed only at loop level in the SM, allowing the explorationg of effects where the dominant tree level is forbidden. Additional new physics that arise from additional particles through virtual loops allow a direct test of heir contributions. Rare decays with FCNCs have been extensively considered in the case of down-type quarks, B, K mesons. The rare decays of these down-type mesons have already provided tight constraints on NP. In the charm sector, the lack of an equivalently heavy down-type quark ($m_t >> m_b$) leads to a greater suppression of SM short distance amplitudes. The rare decays of D mesons therefore are usually dominated by non-perturbative long-distance effects and are more difficult to calculate.

Additional NP can enhance both short and long distance contributions, and in some models can be orders of magnitude larger than the SM [78, 79, 80]. In order to take any constraints on NP seriously it is important to have a very reliable SM prediction.

We consider the SM contribution of two-particle intermediate states to the decay of $D^0 \to \mu^+\mu^-$. This decay is suppressed in the standard model, and still outside of current experimental resolution. The leading contributions are from the unitary contribution of $D^0 \to \gamma\gamma \to \mu^+\mu^-$, and is predicted to be $\mathcal{B}r \approx \mathcal{O}(10^{-13})$ [81]. The short distance $\mathcal{O}(10^{-18})$ and single particle unitary contributions $\mathcal{O}(10^{-17})$ are much smaller [81].

We propose that two-particle unitary contributions may be of significance, and wish to analyze which intermediate states may be involved.

We split the calculation into four parts: The calculation of the hadronic weak decay amplitude of $D \to PP$ and $D \to PV$; the integration over the inner-loop momenta using

Cutkosky rules; the pQCD factorized amplitude of $PP(V) \to \mu^+\mu^-$, and the dispersion relation to obtain both the real and imaginary parts of the amplitude. We will see that many states do not contribute at leading order.

5.2 $SU(3)$ Flavor Decays of Charmed Mesons

While pQCD, SCET and QCD factorization are all applicable to hadronic B decays, the charm case is more difficult. In hadronic decays, the mass of the charm meson, $M_D \approx 1.5GeV$, is too heavy for a proper chiral perturbative expansion and yet too light to create trustworthy heavy quark expansions. Factorization methods fail to properly describe color-suppressed decay modes [82]. If one lets N_c become 'large", the Fierz transformed terms in factorization can be neglected and resolves some of the discrepancy between experiment and theory [83, 84, 85, 86, 87], though this method is not general to both D and B decays.

One valuable method of determining hardronic decay amplitudes of charmed mesons is based on a model-independent diagrammatic expansion. Topological flavor flow diagrams expanded in the weak-interaction allows an experimentally-based parametrical fit that includes all strong interactions. One must assume a base $SU(3)$ flavor symmetry, but broken symmetry effects can be parameterized and fit depending on experimental data.

The diagrammatic approach separates amplitudes into categories of diagrams: Color-allowed amplitudes T; Color-suppressed amplitudes C; W-Exchange amplitudes E, and W-Annhilation amplitudes A. These parameters, as well as relevant strong phases, can be fit currently to experimental data.

We wish to use this approach to model-independently fit both the real and imaginary parts of the intermediate-state amplitudes, $D^0 \to PP(V)$, in order to use with our dispersive amplitude approach. The fits have been done in [82], and while $SU(3)$ breaking effects have been improved in [88], they have not calculated PV amplitudes which are necessary for our calculation.

5.2.1 Amplitudes

The amplitudes are fit using the partial decay width

$$\Gamma(D \to PP) \quad = \quad \frac{p_c}{8\pi M_D^2}|\mathcal{A}|^2. \tag{5.1}$$

For $D^0 \to PP$ we use the parameters, in units of $10^{-6}GeV$ [82]

$$T = 3.14, \qquad C = (2.61)e^{-i(152\pm1)^\circ}, \tag{5.2}$$

$$E = (1.53)e^{i(122\pm2)^\circ}, \qquad A = (0.39)e^{i(31^{+20}_{-33})^\circ}, \tag{5.3}$$

and for the Cabibbo-suppressed decays

$$T' = 1.14, \qquad C' = (2.36)e^{i222^\circ}, \tag{5.4}$$

$$E' = (1.85)e^{-i52^\circ}, \qquad A' = (2.51)e^{i100^\circ}. \tag{5.5}$$

The amplitudes, X_{PP} are given by these are found in Table 5.2.1.

Meson	Mode	Representation	X_{PP}
$D^0 \to$	$\pi^+\pi^-$	$V_{cd}^* V_{ud}\,(T' + E')$	-0.50 + 0.32 i
	$\pi^0\pi^0$	$\frac{1}{\sqrt{2}} V_{cd}^* V_{ud}\,(C' - E')$	0.45 + 0.02 i
	K^+K^-	$V_{cs}^* V_{us}\,(T' + E')$	0.50 - 0.32 i
	$K^0\bar{K}^0$	$V_{cd}^* V_{ud} E_s' + V_{cs}^* V_{us} E_d'$	0 + 0 i

Table 5.2.1: Cabibbo-suppressed Decay Amplitudes X_{PP} in units $10^{-6}GeV$.

The parameters for the PV case are those found in [82] for solutions S and $S1$. These are argued to be the most likely solutions as they have the lowest χ^2 and several of the others are ruled out by additional hadronic decays. They are fit using the partical decay width

definition

$$\Gamma(D \to PV) \quad = \quad \frac{p_c}{8\pi M_D^2} \sum_{pol} |\mathcal{A}|^2, \tag{5.6}$$

where the polarization of the vector meson has been intentionally left in the definition of the amplitude. This yields the best fit parameters

$$\begin{aligned} T_P &= 3.14^{+0.29}_{-0.31}, \qquad C_V = (4.15^{+0.34}_{-0.57})e^{i(177^{+16}_{-13})^\circ}, \qquad E_V = (1.31^{+0.40}_{-0.47})e^{-i(106^{+13}_{-16})^\circ}, \\ T_V &= 2.15^{+0.08}_{-0.09}, \qquad C_P = (2.68^{+0.14}_{-0.15})e^{-i(164\pm3)^\circ}, \qquad E_P = (1.69 \pm 0.06)e^{-i(103\pm4)^\circ}. \end{aligned} \tag{5.7}$$

These result in the hadronic $D^0 \to PV$ amplitudes found in Table 5.2.2.

Meson	Mode	Representation	X_{PP}
$D^0 \to$	$\pi^+\rho^-$	$V_{cd}^* V_{ud}\,(T'_V + E'_P)$	-0.39 + 0.36 i
	$\pi^-\rho^+$	$V_{cd}^* V_{ud}\,(T'_P - E'_V)$	-0.61 + 0.28 i
	K^+K^{*-}	$V_{cs}^* V_{us}\,(T'_V + E'_P)$	0.39 - 0.36 i
	K^-K^{*+}	$V_{cs}^* V_{us}\,(T'_P + E'_V)$	0.61 - 0.28 i

Table 5.2.2: Cabibbo-suppressed Decay Amplitudes X_{PV} in units $10^{-6}(\epsilon \cdot P_D)GeV$.

We now have the complex amplitudes necessary to calculate the dispersive part of the 2PUC amplitude. As we saw in (5.28) only the imaginary component of these amplitudes will contribute due to the nature of the remaining part of the diagram.

5.2.2 pQCD Form Factors

Perturbative QCD [67] is a large field of diverse methods, applications and approximations describing the factorization of hard and soft physics of QCD at high energy scales. We use an elementary version restricted to a leading-order calculation of the neutral-weak transition amplitude of two light mesons. As such, if the reader is interested in the applicability of

pQCD to heavy meson decays or other uses there is an abundance of literature to provide an essential primer [89, 90].

The factorization of an amplitude can be expressed as an intergral over the momentum fractions of the product of the distribution amplitudes(DA) $\phi_{P,V}(x)$ and the hard scattering amplitude (HSA) $T_H(x, y, Q^2)$.

$$\langle P_2| \sum_{q=u,d,s} C_V^q \bar{q}\gamma^\mu q|P_1\rangle_0 \quad = \quad \int_{x,y} \phi_P(x) T_H(x, y, s, \mu^2) \phi_P^\dagger(y), \tag{5.8}$$

where we have defined the variable $s = (p_1 - p_2)^2 = Q^2$, and the notation

$$\int_{x,y} \equiv \int_0^1 dx \int_0^1 dy. \tag{5.9}$$

First we will consider the pQCD calculation of form factors for $PP(V) \to \mu^+\mu^-$ as we will see it sets a limit on which channels contribute and which are zero at leading order. We can generally parameterize matrix elements for vector and axial-vector PP and PV transitions, where $m_2 \geq m_1$ as

$$\begin{aligned}
\langle P(p_2)|\mathcal{J}_V^\mu|P(p_1)\rangle &= f_+^{PP}(q^2)\left[p_1^\mu + p_2^\mu - \frac{m_2^2 - m_1^2}{q^2}q^\mu\right] + f_0^{PP}(q^2)\left[\frac{m_2^2 - m_1^2}{q^2}q^\mu\right] \\
\langle V(p_2)|\mathcal{J}_V^\mu|P(p_1)\rangle &= V^{PV}(q^2)\left[\frac{2}{m_1 + m_2}\,\epsilon^{\mu\nu\alpha\beta} p_{1\nu} p_{2\alpha} \epsilon^*_{2\beta}\right] \\
\langle V(p_2)|\mathcal{J}_A^\mu|P(p_1)\rangle &= iA_1^{PV}(q^2)\left[(m_1 + m_2)\epsilon^*_{2\mu}\right] - iA_2^{PV}(q^2)\left[\frac{(\epsilon_2^* \cdot p_1)}{m_1 + m_2}(p_1^\mu + p_2^\mu)\right] \\
&- i\left(A_3^{PV}(q^2) - A_0^{PV}(q^2)\right)\left[\frac{2m_2}{q^2}(\epsilon_2^* \cdot p_1)q_\mu\right],
\end{aligned} \tag{5.10}$$

where $q = p_1 - p_2$. Using the BSW parameterization [91], where A_0, A_1, A_2, A_3 are related

through

$$A_3^{PV} = \frac{m_1 + m_2}{2m_2} A_1^{PV}(q^2) - \frac{m_1 - m_2}{2m_2} A_2^{PV}(q^2), \tag{5.11}$$

Here it should be noted that in general these form factors will have a contribution from each quark current involved in the process. In our case the neutral currents are flavor-conserving currents of the form $\bar{q}\gamma_\mu q$ and $\bar{q}\gamma_\mu\gamma^5 q$.

The LO electroweak contributions require the sum of the intermediate states to be flavor-neutral, that is to say contributions of the form $D^0 \to K^+\pi^- \to \mu^+\mu^-$ will be neglected, as they will be higher order in G_F due to the electroweak transition required at the leptonic vertex to change flavors. Leading processes will occur through an off-shell Z boson, as conservation of the leptonic vector current eliminates the contribution from an off-shell photon. The amplitude will be helicity suppressed by the lepton mass due to the nature of the decaying particle as explained previously. Thus, only the axial muonic current will contribute.

The hard scattering amplitude can be calculated by the quark-level diagrams as seen in Figure 5.2.1. For both the PP and PV cases there are two groups of diagrams; one for neutral mesons, one for charged mesons.

For neutral initial and final states there are 4 additional diagrams. These annhilation-type diagrams are $\frac{1}{N_c}$ suppressed.

For the charged pseudoscalar meson pairs there are four same-flavor combinations, $\pi^\pm \to \pi^\pm Z^*$ and $K^\pm \to K^\pm Z^*$, that will determine which intermediate states will contribute at leading order. For one pseudoscalar and one vector meson the possible charged combinations are $\pi^\pm \to \rho^\pm Z^*$, $K^\pm \to K^{*\pm} Z^*$. As we're concerned with a rough approximation we take

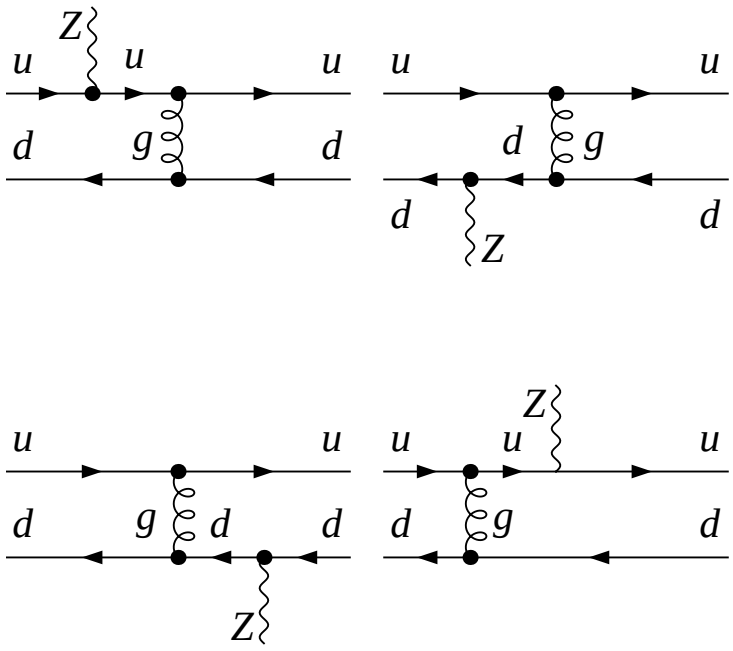

Figure 5.2.1: Quark-flow diagrams contributing to the charged-meson hard scattering amplitude T_H.

the meson wave functions at leading Twist (Twist-2) are defined as [92]

$$\begin{aligned}\Phi_P(P,x) &= \frac{1}{\sqrt{2N_c}}\gamma_5 \not{P}\phi_P(x),\\ \Phi_V(P,\eta,x) &= \frac{1}{\sqrt{2N_c}} \not{\epsilon}_L M_V \phi_{V_L}(x),\end{aligned} \tag{5.12}$$

where only the longitudinal component of the vector meson participates at Twist-2. The parton distribution functions are defined as an expansion in Gegenbauer polynomials and are [92]

$$\begin{aligned}\phi_P(x) &= \frac{f_P}{2\sqrt{2N_c}} 6x(1-x)(1+a_{2P}C_2^{\frac{3}{2}}[2x-1]+a_{4P}C_4^{\frac{3}{2}}[2x-1]),\\ \phi_{V_L}(x) &= \frac{f_{V_L}}{2\sqrt{2N_c}} 6x(1-x)(1+a_{2V}C_2^{\frac{3}{2}}[2x-1]).\end{aligned} \tag{5.13}$$

Here we use the numerical values $a_{2\pi} = 0.35$, $a_{4\pi} = -0.015$, $a_{2K} = 0.35$, $a_{4K} = 0$, $a_{2\rho} = 0.15$, $a_{2K^*} = 0.18$ [93, 94].

The Gegenbauer polynomials used are defined as

$$\begin{aligned} C_1^{\frac{3}{2}}[t] &= 3t, \qquad (5.14) \\ C_2^{\frac{3}{2}}[t] &= \frac{3}{2}(5t^2-1), \qquad (5.15) \\ C_4^{\frac{3}{2}}[t] &= \frac{15}{8}(21t^4-14t^2+1). \end{aligned}$$

PP

Using the above with the hard scattering amplitude we obtain our LO matrix element for a PP current coupling a SM vector current,

$$\begin{aligned} \langle P_2| \sum_{q=u,d,s} C_V^q \bar{q}\gamma^\mu q|P_1\rangle_0 &= \int_{x,y} \phi_P(x) T_H(x,y,s,\mu^2) \phi_P^\dagger(y) \qquad (5.16) \\ &= \frac{16\pi\alpha_s(\mu^2)C_F(C_V^u - C_V^d)}{s}(P_1^\mu + P_2^\mu)\int_{x,y}\frac{\phi_P(x)\phi_P^\dagger(y)}{xy} \end{aligned}$$

which is very simply related to the leading order form factor, f_+^{PP} in (5.10). Here $C_F = \frac{N_c^2-1}{2N_c}$ and the number of colors $N_c = 3$. C_V^q are the vector component coefficients of the standard model neutral current. These are listed in Table 5.2.3.

q	C_V^q	C_A^q
u	$i\frac{g_W\left(3-8\sin^2\theta_W\right)}{12\cos\theta_W}$	$-i\frac{g_W}{4\cos\theta_W}$
d/s	$i\frac{g_W\left(4\sin^2\theta_W-3\right)}{12\cos\theta_W}$	$i\frac{g_W}{4\cos\theta_W}$
e/μ	$i\frac{g_W\left(\sin^2\theta_W-\frac{1}{4}\right)}{\cos\theta_W}$	$i\frac{g_W}{4\cos\theta_W}$

Table 5.2.3: SM vector and axial-vector neutral current coefficients

Integrating over the momentum fractions using the definitions in (5.13) we have

$$f_+^{PPZ}(s) \quad = \quad \frac{18\pi\alpha_s(\mu^2) f_{P_1} f_{P_2} C_F (C_V^u - C_V^d)}{N_c} \frac{1}{s}, \tag{5.17}$$

The pseudoscalar-vector coupling is a touch more difficult, as at first glance it involves end-point divergences. This can be resolved by threshold resummation insertion which smears out the endpoints, allowing a rough calculation.

PV And Threshold Resummation

We use the method of [95] of inserting a threshold resummation factor,

$$S_t(x,Q) \quad = \quad \frac{2^{1+2c}\Gamma(3/2+c)}{\sqrt{\pi}\Gamma(1+c)}[x(1-x)]^c, \tag{5.18}$$

$$\int_{x,y} \phi(x) T_H(x,y,Q^2) \phi^\dagger(y) \quad \rightarrow \quad \int_{x,y} \phi(x) S(x,c) T_H(x,y,Q^2) S(y,c) \phi^\dagger(y) \tag{5.19}$$

This factor was derived in [96] at the scale of $M_B 5.28 GeV$, and is phenomenologically motivated. We must modify its power-law behavior as for our case $Q^2 = M_{D^0} \approx (1860 GeV)^2$. This method has been first given in [96], where [97] derived the parabolic parameterization

$$c \rightarrow c(Q^2) = max(0.04Q^2 - 0.51Q + 1.87,\, 1\,). \tag{5.20}$$

where for our case $c \rightarrow 1$. This provides a quick falloff as $x \rightarrow 0$ which removes the divergence by spreading out the endpoint divergence without the need for Sudakov resummation factors.

Following the same method as before and integrating with the the threshold resummation

factor we have the vector form factor

$$\begin{aligned} V^{PV}(s) &= \left(8i\pi\alpha_s(\mu^2)C_F m_2\right)(m_1+m_2)(C_V^u+C_V^d) \\ &\times \int_{x,y}\phi_P(x)S(x,c)\left(\frac{x-1}{x^2ys^2}\right)S(y,c)\phi_V^\dagger(y) \\ &= (32.13)i\frac{\pi\alpha_s(\mu^2)f_{P_1}f_{V_{2L}}m_2(m_1+m_2)C_F(C_V^u+C_V^d)}{N_c}\frac{1}{s^2}. \end{aligned} \tag{5.21}$$

The axial form factors are

$$\begin{aligned} A_1^{PV}(s) &= -\left(8i\pi\alpha_s(\mu^2)C_F\frac{m_2}{m_1+m_2}\right)(C_A^u-C_A^d) \\ &\times \int_{x,y}\phi_P(x)S(x,c)\left(\frac{1+x}{x^2ys}\right)S(y,c)\phi_V^\dagger(y) \\ &= (50.13)i\frac{\pi\alpha_s(\mu^2)f_{P_1}f_{V_{2L}}m_2(m_1+m_2)C_F(C_A^u+C_A^d)}{N_c}\frac{1}{s}, \end{aligned} \tag{5.22}$$

$$\begin{aligned} A_2^{PV}(s) &= \left(4i\pi\alpha_s(\mu^2)C_F m_2(m_1+m_2)\right)(C_A^u+C_A^d) \\ &\times \int_{x,y}\phi_P(x)S(x,c)\left(\frac{1-3x}{x^2ys^2}\right)S(y,c)\phi_V^\dagger(y) \\ &= (7.065)i\frac{\pi\alpha_s(\mu^2)f_{P_1}f_{V_{2L}}m_2(m_1+m_2)C_F(C_A^u-C_A^d)}{N_c}\frac{1}{s^2}, \end{aligned} \tag{5.23}$$

$$\begin{aligned} A_3^{PV}(s) &= -\left(2i\pi\alpha_s(\mu^2)C_F(C_A^u-C_A^d)\right) \\ &\times \int_{x,y}\phi_P(x)S(x,c)\left(\frac{(2s(x+1)-(1-3x)(m_2^2-m_1^2)}{x^2ys^2}\right)S(y,c)\phi_V^\dagger(y) \\ &= -(3.53)i\frac{\pi\alpha_s(\mu^2)f_{P_1}f_{V_{2L}}C_F(C_A^u-C_A^d)}{N_c}\frac{5.82s-(m_2^2-m_1^2)}{s^2}, \end{aligned} \tag{5.24}$$

$$
\begin{aligned}
A_0^{PV}(s) &= -\left(2i\pi\alpha_s(\mu^2)C_F(C_A^u - C_A^d)\right) \\
&\times \int_{x,y} \phi_P(x)S(x,c)\left(\frac{(m_1^2(1-3x)+m_2^2(3x-1)+sx+s)}{x^2ys^2}\right)S(y,c)\phi_V^\dagger(y) \\
&= -(3.53)i\frac{\pi\alpha_s(\mu^2)f_{P_1}f_{V_{2L}}C_F(C_A^u - C_A^d)}{N_c}\frac{3.53s-(m_2^2-m_1^2)}{s^2}, \qquad (5.25)
\end{aligned}
$$

5.2.3 Application

We now turn to the application of the Cutkosky rules to our amplitude. We set up our momenta as seen in Fig. 5.2.2, with the loop integral over the momentum p_1.

The absorptive part of our diagram then comes from a cut across the intermediate states, putting both mesons on mass shell and moving in the forward direction. Here we must be careful when calculating the absorptive part. We want only the imaginary contributions to this diagram, and while Cutkosky rules are correct, we must remember that both of the $D \to PP(V)$ and $PP(V) \to \mu^+\mu^-$ vertices may be complex. If we take only the imaginary part of the propagators, when they're both on-shell, we will have something real times two complex numbers.

He were argue that for the $PP(V) \to \mu^+\mu^-$ amplitude, we can ignore the real contributions; the PP case only has an imaginary component while the PV case has both. In the PV case, the real component is due to the form factor $V(q^2)$ only which is anti-symmetric in indices. The first amplitude in our case only has one degree of freedom : $\mathcal{M}(D \to PV) \propto P_D \cdot \epsilon_V$, and so after performing the multiplication will remove the $V(q^2)$ term. This leaves the PV case also only imaginary. It should be pointed out that if we were considering the decay of a vector particle, D^*, there would be an additional term from the product of the vector pQCD form factor and the real part of the hadronic matrix element.

The amplitude of $D \to PP(V)$, from the $SU(3)$ flavor fit has both real and imaginary

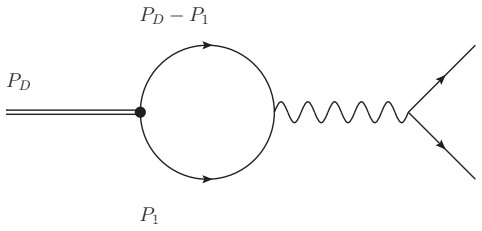

Figure 5.2.2: Forward momentum configuration for loop integral.

parts. With

$$\begin{aligned} \mathcal{M}(D^0 \to PP(V)) &= (R_1 + iI_1), \\ \mathcal{M}(PP(V) \to \mu^+\mu^-) &= (R_2 + iI_2) \Rightarrow iI_2, \\ \int \frac{d^4p_2}{(2\pi)^4} \frac{i}{p_2^2 - m_2^2 + i\epsilon} \frac{i}{(P_D - p_2)^2 - m_1^2 + i\epsilon} &= i^2(Re[L] + iIm[L]). \end{aligned} \tag{5.26}$$

We wish to calculate the product of the above, with a Hermitian conjugate on the second equation. Then we can choose our cutting rules to result in the imaginary part.

$$\begin{aligned} iIm[\mathcal{M}(D^0 \to PP(V) \to \mu^+\mu^-)] &= (R_1 + iI_1)(iI_2)^\dagger i^2(Re[L] + iIm[L]), \\ &= (iR_1I_2 - I_1I_2)(Re[L] + iIm[L]), \\ &= i(R_1I_2Re[L] - I_1I_2Im[L]), \end{aligned} \tag{5.27}$$

where we have ignored real contributions. Due to the complex nature of the decay amplitude we must also consider whether or not the real part of the propagators will participate. This is of course easy, as one can argue that the real part of a propagator only occurs when the momenta are off-shell. Once off-shell, there are no poles, and so they are completely real. If you perform a Wick rotation on the propagators you will pick up an extra i, thus making them imaginary. This means they must be zero. Our end result is

$$Im[\mathcal{M}(D^0 \to PP(V) \to \mu^+\mu^-)] = -I_1I_2Im[L]. \tag{5.28}$$

We now use Cutkosky rules to cut across both propagators, putting them on-shell with the replacement

$$\frac{1}{p^2 - m^2 + i\epsilon} \to -i\pi\delta\left(p^2 - m^2\right)\Theta[p^0]. \tag{5.29}$$

we can put our propagators on mass shell,

$$\begin{aligned}\frac{1}{p_2^2 - m_2^2 + i\epsilon}\frac{1}{p_1^2 - m_1^2 + i\epsilon} \to \\ \left(-i\pi\delta\left(p_2^2 - m_2^2\right)\Theta[E_2]\right) \quad \left(-i\pi\delta\left((P_D - p_2)^2 - m_1^2\right)\Theta[\sqrt{s} - E_2]\right).\end{aligned} \tag{5.30}$$

We have forced positive energy solutions only with the Heaviside Theta function, Θ. We can simplify the loop integral with the customary replacements

$$\begin{aligned}\frac{d^4p_2}{(2\pi)^4}\delta\left(p_2^2 - m_2^2\right)\Theta(E_2) &= \frac{1}{(2\pi)^4}\frac{d^3p_2}{2E_2}, \\ &= \frac{1}{(2\pi)^4}\frac{1}{2}d\Omega_2\sqrt{E_2^2 - m_2^2}dE_2.\end{aligned} \tag{5.31}$$

We now consider each case, $D \to PP, D \to PV$ respectively.

$D \to PP$

In the case of pseudoscalar mesons consisting of one up-type and one down-type quark we can write the amplitude including the electroweak neutral coupling constants,

$$\begin{aligned}Im[\mathcal{M}(D^0 \to PP \to \mu^+\mu^-)] &= \frac{Im[\mathcal{M}(D^0 \to PP]}{(2\pi)^4}\frac{1}{2}\int d\Omega_2 \int dE_2\sqrt{E_2^2 - m_2^2} \\ &\times \left(\int_0^1 dx \int_0^1 dy \frac{\phi_P(x)\phi_P(y)}{xy}\right) \\ &\times (-4\pi\alpha_S g_W)\frac{(N_c^2 - 1)}{N_c^2}\frac{2\sin^2\theta_W - 1}{\cos\theta_W}\frac{1}{s} \\ &\times (p_1^\mu - p_2^\mu)\frac{ig_{\mu\nu}}{M_Z^2}[\bar{u}iC_A^\ell\gamma^\nu\gamma^5 u].\end{aligned} \tag{5.32}$$

Again we recall that only the axial muonic current will participate due to conservation of the vector current. Rather than perform this calculation completely, we look specifically at the integral over the loop energy and angle first.

Defining

$$p_2^\mu = \sqrt{E_2^2 - m_2^2}\left\{\frac{E_2}{\sqrt{E_2^2 - m_2^2}},\, \sin\theta\sin\phi,\, \sin\theta\cos\phi,\, \cos\theta\right\},$$
$$p_1^\mu = \sqrt{s}\left\{1,\, 0,\, 0,\, 0\right\} - p_2^\mu, \tag{5.33}$$

we see that the integration over energy and momenta leads to

$$\int_{E_2}\int_{\Omega_2}(p_1 - p_2)^\mu \propto \left(m_1^2 - m_2^2\right). \tag{5.34}$$

Rather than go further we recall that the only contributing pairs at leading order in the electroweak expansion are those that have matching pairs of quark flavors, $\pi^\pm\pi^\mp, K^\pm K^\mp$, which are degenerate in mass. Additionally, neutral combinations that have non-degenerate mass do not contribute as at leading order all diagrams cancel. This makes sense as at tree level the Z-charge of neutral mesons is zero. This argument will hold for PV states as well. Thus contributions from all PP states can be ignored for further calculation. While this seems like a null result, it allowed us to have the simple framework to compute the PV contributions, where no mass degeneracy exists, and the δm is actually large.

$D \to PV$

The calculation for PV intermediate states is very similar to the PP case. The first difference we need to address is the vector meson propagator. We recall from the pQCD discussion that at the leading twist-2 expansion the wavefunction for a light vector meson has only the longitudinal component. This means that rather than sum over all helicities in the propagator we will only sum over the longitudinal polarization, ϵ_3^μ which we define for

V being particle 2 as

$$\epsilon_3^\mu = \frac{E_2}{m_2}\{\frac{\sqrt{E_2^2-m_2^2}}{E_2}, \sin\theta\sin\phi, \sin\theta\cos\phi, \cos\theta\}, \tag{5.35}$$

still satisfying $p_2 \cdot \epsilon_3 = 0$. The amplitude for $D \to PV$ is again parameterized by

$$\begin{aligned}\mathcal{M}(D^0 \to PV) &= (R_1^{PV} + iI_1^{PV})(P_D \cdot \epsilon_V), \\ &= (R_1^{PV} + iI_1^{PV})(p_1 \cdot \sum_{i=1,2,3} \epsilon_{V_2 i}),\end{aligned} \tag{5.36}$$

where we have summed over polarizations. Using (5.33) and (5.35) we have

$$p_1 \cdot \epsilon_{V_2 3} = \frac{\sqrt{s\,(E_2^2-m_2^2)}}{m_2}. \tag{5.37}$$

The simplest way to compute the integral is to separate the $PV \to \mu^+\mu^-$ amplitude not into the normal form factors but rather just into the momentum dependent parts, knowing that the leptonic current, L_μ, will not be dependent on the internal momentum. We ignore the vector form factor (Levi Civita term) as it does not contribute (and actually integrates to zero), and $p_2 \cdot \epsilon_3 = 0$ to limit our terms.

The explicit momentum dependence of our amplitude allows us to integrate over the internal loop momentum and angles, giving the replacements

$$\int_{E_2}\int_{\Omega_2} (p_1 \cdot \epsilon_3)\epsilon_3^\mu = \frac{|\vec{P}_{12}|^3}{4\pi m_2^2\sqrt{s}} P_D^\mu, \tag{5.38}$$

$$\int_{E_2}\int_{\Omega_2} (p_1 \cdot \epsilon_3) p_1^\mu\,(p_1 \cdot \epsilon_3) = \frac{|\vec{P}_{12}|^3(s - m_1^2 + m_2^2)}{8\pi m_2^2\sqrt{s}} P_D^\mu, \tag{5.39}$$

$$\int_{E_2}\int_{\Omega_2} (p_1 \cdot \epsilon_3)\; p_2^\mu\,(p_1 \cdot \epsilon_3) = \frac{|\vec{P}_{12}|^3(s + m_1^2 - m_2^2}{4\pi m_2^2\sqrt{s}} P_D^\mu, \tag{5.40}$$

where we have defined

$$|\vec{P}_{12}| = \frac{\sqrt{(s-(m_1+m_2)^2)(s-(m_1-m_2)^2)}}{2\sqrt{s}}. \tag{5.41}$$

Integration over x, y is trivial and our end result for the non-leptonic part of the decay amplitude with $N_c = 3$,

$$2\,\mathcal{I}m[\mathcal{A}(D^0 \to \mu^+\mu^-)_{PV}] = (18.28)\frac{\pi\alpha\mu^2 f_P f_{V_L} m_\ell |\vec{P}_{12}|^3 (m_2^2 - m_1^2)}{m_2 m_Z^2}(C_A^u - C_A^d)C_A^\ell \frac{1}{s^2}. \tag{5.42}$$

We have used the large-mass Z boson propagator $ig^{\mu\nu}/M_Z^2$, and resolved the leptonic axial current into helicity states. This allows us two possible relative helicity contributions to the amplitude. With constructing the D^0 momenta from

$$\begin{aligned} v^\mu[\bar{u}_1\gamma_\mu\gamma^5 v_2] &= \frac{1}{\sqrt{s}}P_D^\mu[\bar{u}_1\gamma_\mu\gamma^5 v_2], \\ &= 2\frac{m_\mu}{\sqrt{s}}[\bar{u}_1\gamma_\mu\gamma^5 v_2], \\ &= 2\frac{m_\mu}{\sqrt{s}}(\sqrt{s}\,(\delta_{\uparrow\uparrow} + \delta_{\downarrow\downarrow})\,, \\ &= 2m_\mu \times \sqrt{2}, \end{aligned} \tag{5.43}$$

where in the last line we have used the fact that the sum over helicity states will give us a factor of 2 in the final decay width. We expand our amplitude in mass of the lighter meson, though we keep the first order correction. Our dispersive integral becomes

$$\mathcal{A}(D^0 \to \mu^+\mu^-)_{PV} = \frac{1}{\pi}\int_{(m_1+m_2)^2}^{\infty} \frac{ds}{s - M_D^2 - i\epsilon}\mathcal{I}m[\mathcal{A}(D^0 \to \mu^+\mu^-)_{PV}] \tag{5.44}$$

We use the masses and decay constants listed in Figure 5.2.3 [98], in addition to the 2012 PDG [59] for universal constants and CKM matrix parameters.

$m_{\pi^\pm}$	$139.6MeV$	f_π	$130MeV$
$m_{\rho^\pm}$	$775.5MeV$	f_ρ^L	$216MeV$
$m_{K^\pm}$	$493.7MeV$	$f_{K^\pm}$	$156MeV$
$m_{K^{*\pm}}$	$891.7MeV$	$f_{K^{*\pm}}^L$	$220MeV$
m_{D^0}	$1865.9MeV$	m_μ	$105MeV$

Figure 5.2.3: Meson masses and decay constants

The width if the D^0 meson is [59]

$$\Gamma(D^0) \quad = \quad 1.605 \times 10^{-9} MeV. \tag{5.45}$$

The sum of our numerical amplitudes is

$$\mathcal{A}(D^0 \to \mu^+\mu^-)_{PV} \quad = \quad (-2.8 + 5.6i) \times 10^{-11} MeV, \tag{5.46}$$

giving a branching ratio of

$$\mathcal{B}r(D^0 \to \mu^+\mu^-)_{PV} \approx 2 \times 10^{-17}. \tag{5.47}$$

Discussion

While $\mathcal{O}(10^{-17})$ is small compared to the leading di-photon contribution $\mathcal{O}(10^{-13})$, it is is larger than all other sub-leading contributions. It has been argued for the pion-photon transition at low-Q^2 that NLO calculations have considerable corrections [99]. Additionally, our calculation was only LO in $SU(3)$ violation for the $D \to P(V)$ amplitudes, as a fit to experimental data has not been performed for PV cases, though it has for PP. Our amplitude is proportional to the $SU(3)$ violation, and thus any improvement may drastically increase the result. It would be beneficial then to improve both the pQCD transition form factors by increasing the NLO hard scattering amplitude as well as twist-3 wavefunctions.

Due to the contributions at the wavefunction endpoints there may be large corrective effects.

CHAPTER 6

SUMMARY

In this doctoral dissertation I have discussed the possible standard model contributions to select leptonic heavy meson decay modes. We calculated a $1-3\%$ increase in $B_s \to \mu^+\mu^-$ from soft photon contributions through select vector resonances is a nearly model-independent method. We have computed constraints for two super-WIMP dark matter models from the rare leptonic decays of heavy mesons. While these are not as tight as constraints from new physics, tighter experimental bounds will allow our calculation to be refit. Finally I calculated a previously unmentioned two-meson unitary contribution to the rare decay $D^0 \to \mu^+\mu^-$ as well as calculated LO form factors for $P \to PZ$ and $P \to VZ$ light charged mesons. This contribution is $\mathcal{O}(10^{-17})$ while the leading order gamma-gamma contribution is $\mathcal{O}(10^{-13})$. I believe this work can be continued and a larger contribution may unfold once the $SU(3)$ violating effects in the PV intermediate state are better fit. Additionally, a higher-twist and NLO QCD expansion may provide a better description of the $P \to VZ$ form factors.

APPENDIX

Channel (Seen)	Experiment (Maximum)	Standard Model	$f_a^2 R_a(E_0)$ $E_0 = 100$ MeV	$R_{\gamma_s}(E_0')$ $E_0' = 50$ MeV	$R_{\gamma_s}(E_0')$ $E_0' = 100$ MeV	$R_{\gamma_s}(E_0')$ $E_0' = 300$ MeV
$\mathcal{B}\left(B^{\pm} \to \tau^{\pm}\bar{\nu}_{\tau}\right)$	1.7×10^{-4}	7.9×10^{-5}	1.6×10^{2}	4.9×10^{-5}	1.9×10^{-4}	1.9×10^{-3}
$\mathcal{B}\left(D^{\pm} \to \mu^{\pm}\bar{\nu}_{\mu}\right)$	3.8×10^{-4}	3.6×10^{-4}	3.1×10^{3}	4.0×10^{-3}	1.8×10^{-2}	1.7×10^{-2}
$\mathcal{B}\left(D_s^{\pm} \to \mu^{\pm}\bar{\nu}_{\mu}\right)$	5.9×10^{-3}	5.3×10^{-3}	4.6×10^{2}	2.0×10^{-4}	7.8×10^{-4}	6.0×10^{-3}
$\mathcal{B}\left(D_s^{\pm} \to \tau^{\pm}\bar{\nu}_{\tau}\right)$	5.4×10^{-2}	5.1×10^{-2}	6.5×10^{0}	2.1×10^{-5}	8.0×10^{-5}	6.2×10^{-4}
Channel (Unseen)						
$\mathcal{B}\left(B^{\pm} \to e^{\pm}\bar{\nu}_{e}\right)$	$< 1.9 \times 10^{-6}$	8.3×10^{-12}	6.6×10^{7}	4.6×10^{2}	1.8×10^{3}	1.6×10^{4}
$\mathcal{B}\left(B^{\pm} \to \mu^{\pm}\bar{\nu}_{\mu}\right)$	$< 1.0 \times 10^{-6}$	3.5×10^{-7}	1.8×10^{3}	1.1×10^{-2}	4.3×10^{-2}	3.6×10^{-1}
$\mathcal{B}\left(D^{\pm} \to e^{\pm}\bar{\nu}_{e}\right)$	$< 8.8 \times 10^{-6}$	8.5×10^{-9}	3.1×10^{6}	1.9×10^{2}	7.6×10^{2}	7.1×10^{3}
$\mathcal{B}\left(D^{\pm} \to \tau^{\pm}\bar{\nu}_{\tau}\right)$	$< 1.2 \times 10^{-3}$	9.7×10^{-4}	1.0×10^{1}	1.7×10^{-3}	7.7×10^{-3}	6.2×10^{-2}
$\mathcal{B}\left(D_s^{\pm} \to e^{\pm}\bar{\nu}_{e}\right)$	$< 1.2 \times 10^{-4}$	1.2×10^{-7}	9.8×10^{6}	8.6×10^{0}	3.3×10^{1}	2.6×10^{2}

Table 6.0.1: Constraints on f_a from various decays. The last three columns represent possible soft photon pollution of $M \to \ell\bar{\nu}_{\ell}$ decays for three different values of photon energy cutoff.

REFERENCES

[1] Planck Collaboration, Ade, P.A.R. and others (2013), arXiv: 1303.5062.

[2] WMAP Collaboration, Hinshaw, G. and others (2012), arXiv: 1212.5226.

[3] Glashow, S.L. (1961), Nucl.Phys. 22 579.

[4] Weinberg, Steven (1967), Phys.Rev.Lett. 19 1264.

[5] Glashow, Sheldon L. and Weinberg, Steven (1977), Phys.Rev. D15 1958.

[6] Higgs, Peter W. (1964), Phys.Rev.Lett. 13 508.

[7] Englert, F. and Brout, R. (1964), Phys.Rev.Lett. 13 321.

[8] Guralnik, G.S. and Hagen, C.R. and Kibble, T.W.B. (1964), Phys.Rev.Lett. 13 585.

[9] Stueckelberg, E.C.G. and Petermann, A. (1953), Helv.Phys.Acta 26 499.

[10] Gross, D.J. and Wilczek, Frank (1973), Phys.Rev.Lett. 30 1343.

[11] Jungman, Gerard and Kamionkowski, Marc and Griest, Kim (1996), Phys.Rept. 267 195, hep-ph/9506380.

[12] Bertone, Gianfranco and Hooper, Dan and Silk, Joseph (2005), Phys.Rept. 405 279, hep-ph/0404175.

[13] Zwicky, F. (1933), Helv.Phys.Acta 6 110.

[14] Rubin, Vera C. and Ford, W. Kent, Jr. (1970), Astrophys.J. 159 379.

[15] Rubin, V.C. and Thonnard, N. and Ford, W.K., Jr. (1980), Astrophys.J. 238 471.

[16] WMAP Collaboration, Komatsu, E. and others (2011), Astrophys.J.Suppl. 192 18, arXiv: 1001.4538.

[17] Allen, S.W. and Fabian, A.C. and Schmidt, R.W. and Ebeling, H. (2003), Mon.Not.Roy.Astron.Soc. 342 287, astro-ph/0208394.

[18] Buckley, Matthew R. and Hooper, Dan and Tait, Tim M.P. (2011), Phys.Lett. B702 216, arXiv: 1011.1499.

[19] XENON100 Collaboration, Aprile, E. and others (2011), Phys.Rev.Lett. 107 131302, arXiv: 1104.2549.

[20] Pospelov, Maxim and Ritz, Adam and Voloshin, Mikhail B. (2008), Phys.Rev. D78 115012, arXiv: 0807.3279.

[21] Pospelov, Maxim and Ritz, Adam and Voloshin, Mikhail B. (2008), Phys.Lett. B662 53, arXiv: 0711.4866.

[22] Feng, Jonathan L. and Rajaraman, Arvind and Takayama, Fumihiro (2003), Phys.Rev.Lett. 91 011302, hep-ph/0302215.

[23] Feng, Jonathan L. and Rajaraman, Arvind and Takayama, Fumihiro (2003), Phys.Rev. D68 063504, hep-ph/0306024.

[24] Batell, Brian and Pospelov, Maxim and Ritz, Adam (2009), Phys.Rev. D79 115008, arXiv: 0903.0363.

[25] Essig, Rouven and Kaplan, Jared and Schuster, Philip and Toro, Natalia (2010), Submitted to Physical Review D , arXiv: 1004.0691.

[26] Badin, Andriy and Petrov, Alexey A (2010), Phys.Rev. D82 034005, arXiv: 1005.1277.

[27] Aditya, Y.G. and Healey, K.J. and Petrov, Alexey A. (2013), Phys. Rev. D87 074028, arXiv: 1212.4166.

[28] Aditya, Y.G. and Healey, Kristopher J. and Petrov, Alexey A. (2012), Phys.Lett. B710 118, arXiv: 1201.1007.

[29] Wilson, Kenneth G. (1965) , LNS Publication LNS-64-15 ETC. .

[30] Casalbuoni, R. and Deandrea, A. and Di Bartolomeo, N. and Gatto, Raoul and Feruglio, F. and others (1997), Phys.Rept. 281 145, hep-ph/9605342.

[31] Holstein, Barry R. (2001), Nucl.Phys. A689 135, nucl-th/0010015.

[32] Gasser, J. and Leutwyler, H. (1984), Annals Phys. 158 142.

[33] Grozin, A.G. (1992), hep-ph/9908366.

[34] Wise, Mark B. (1993), hep-ph/9306277.

[35] Stewart, Iain W. (1998), Nucl.Phys. B529 62, hep-ph/9803227.

[36] Kniehl, Bernd A. (1996), Acta Phys.Polon. B27 3631, hep-ph/9607255.

[37] Cutkosky, R.E. (1960), J.Math.Phys. 1 429.

[38] Golowich, Eugene and Hewett, JoAnne and Pakvasa, Sandip and Petrov, Alexey A and Yeghiyan, Gagik K (2011), Phys.Rev. D83 114017, arXiv: 1102.0009.

[39] CDF Collaboration, Aaltonen, T. and others (2011), Phys.Rev.Lett. 107 191801, arXiv: 1107.2304.

[40] Buras, Andrzej J. and Girrbach, Jennifer and Guadagnoli, Diego and Isidori, Gino (2012), Eur.Phys.J. C72 2172, arXiv: 1208.0934.

[41] HPQCD Collaboration, Shigemitsu, J. and others (2009), PoS LAT2009 251, arXiv: 0910.4131.

[42] Buras, Andrzej J. and Jamin, Matthias and Lautenbacher, M.E. and Weisz, Peter H. (1992), Nucl.Phys. B370 69.

[43] Melikhov, Dmitri and Nikitin, Nikolai (2004), Phys.Rev. D70 114028, hep-ph/0410146.

[44] Becirevic, Damir and Haas, Benjamin and Kou, Emi (2009), Phys.Lett. B681 257, arXiv: 0907.1845.

[45] Burdman, Gustavo and Goldman, J. Terrance and Wyler, Daniel (1995), Phys.Rev. D51 111, hep-ph/9405425.

[46] Chiladze, George and Falk, Adam F. and Petrov, Alexey A. (1999), Phys.Rev. D60 034011, hep-ph/9811405.

[47] Wang, Wenyu and Xiong, Zhao-Hua and Zhou, Si-Hong (2013), arXiv: 1303.0660.

[48] Chen, Jun-Xiao and Hou, Zhao-Yu and Lu, Cai-Dian (2007), Commun.Theor.Phys. 47 299, hep-ph/0611245.

[49] Dincer, Yusuf and Sehgal, Lalit M. (2001), Phys.Lett. B521 7, hep-ph/0108144.

[50] Eilam, Gad and Lu, Cai-Dian and Zhang, Da-Xin (1997), Phys.Lett. B391 461, hep-ph/9606444.

[51] Wise, Mark B. (1992), Phys.Rev. D45 2188.

[52] Burdman, Gustavo and Donoghue, John F. (1992), Phys.Lett. B280 287.

[53] Isgur, Nathan and Wise, Mark B. (1990), Phys.Rev. D41 151.

[54] Georgi, Howard (1990), Phys.Lett. B240 447.

[55] Amundson, James F. and Boyd, C. Glenn and Jenkins, Elizabeth Ellen and Luke, Michael E. and Manohar, Aneesh V. (1992), Phys.Lett. B296 415, hep-ph/9209241.

[56] Godang, Romulus (2013), arXiv: 1301.0141.

[57] Aliev, T.M. and Pak, N.K. and Savci, M. (1998), Phys.Lett. B424 175, hep-ph/9710304.

[58] Grinstein, Benjamin and Savage, Martin J. and Wise, Mark B. (1989), Nucl.Phys. B319 271.

[59] Particle Data Group, Beringer, J. and others (2012), Phys.Rev. D86 010001.

[60] Na, Heechang and Monahan, Chris and Davies, Christine and Follana, Eduardo and Horgan, Ron and others (2012), PoS LATTICE2012 102, arXiv: 1212.0586.

[61] Axelrod, Alan (1984), Phys.Rev. D29 2027.

[62] Rosner, Jonathan L. and Stone, Sheldon (2010), arXiv: 1002.1655.

[63] Davies, C.T.H. and McNeile, C. and Follana, E. and Lepage, G.P. and Na, H. and others (2010), Phys.Rev. D82 114504, arXiv: 1008.4018.

[64] Dobrescu, Bogdan A. and Kronfeld, Andreas S. (2008), Phys.Rev.Lett. 100 241802, arXiv: 0803.0512.

[65] Artuso, Marina and Meadows, Brian and Petrov, Alexey A. (2008), Ann.Rev.Nucl.Part.Sci. 58 249, arXiv: 0802.2934.

[66] Szczepaniak, Adam and Henley, Ernest M. and Brodsky, Stanley J. (1990), Phys.Lett. B243 287.

[67] Lepage, G. Peter and Brodsky, Stanley J. (1980), Phys.Rev. D22 2157.

[68] Chang, Chao-Hsi and Cheng, Jian-Ping and Lu, Cai-Dian (1998), Phys.Lett. B425 166, hep-ph/9712325.

[69] Lu, Cai-Dian and Song, Ge-Liang (2003), Phys.Lett. B562 75, hep-ph/0212363.

[70] Heavy Flavor Averaging Group, Asner, D. and others (2010), arXiv: 1010.1589.

[71] Particle Data Group, Nakamura, K. and others (2010), J.Phys. G37 075021.

[72] Lucha, Wolfgang and Melikhov, Dmitri and Simula, Silvano (2010), PoS QFTHEP2010 058, arXiv: 1011.3723.

[73] Scadron, M.D. and Delbourgo, Robert and Rupp, G. (2006), J.Phys. G32 735, hep-ph/0603196.

[74] Nomura, Yasunori and Thaler, Jesse (2009), Phys.Rev. D79 075008, arXiv: 0810.5397.

[75] Freytsis, Marat and Ligeti, Zoltan and Thaler, Jesse (2010), Phys.Rev. D81 034001, arXiv: 0911.5355.

[76] Branco, G.C. and Ferreira, P.M. and Lavoura, L. and Rebelo, M.N. and Sher, Marc and others (2012), Phys.Rept. 516 1, arXiv: 1106.0034.

[77] Blechman, Andrew E. and Petrov, Alexey A. and Yeghiyan, Gagik (2010), JHEP 1011 075, arXiv: 1009.1612.

[78] Fajfer, Svjetlana and Prelovsek, Sasa (2006), Phys.Rev. D73 054026, hep-ph/0511048.

[79] Lee, Jae Yong (2004), JHEP 0412 065, hep-ph/0408362.

[80] Fajfer, Svjetlana and Kosnik, Nejc (2009), Phys.Rev. D79 017502, arXiv: 0810.4858.

[81] Burdman, Gustavo and Golowich, Eugene and Hewett, JoAnne L. and Pakvasa, Sandip (2002), Phys.Rev. D66 014009, hep-ph/0112235.

[82] Cheng, Hai-Yang and Chiang, Cheng-Wei (2010), Phys.Rev. D81 074021, arXiv: 1001.0987.

[83] Tadic, Dubravko and Trampetic, Josip (1982), Phys.Lett. B114 179.

[84] Bauer, Manfred and Stech, Berthold (1985), Phys.Lett. B152 380.

[85] Buras, A.J. and Gerard, J.M. and Ruckl, R. (1986), Nucl.Phys. B268 16.

[86] Blok, B. Yu. and Shifman, Mikhail A. (1987), Sov.J.Nucl.Phys. 45 135.

[87] Fukugita, M. and Inami, T. and Sakai, N. and Yazaki, S. (1977), Phys.Lett. B72 237.

[88] Cheng, Hai-Yang and Chiang, Cheng-Wei (2012), Phys.Rev. D86 014014, arXiv: 1205.0580.

[89] Keum, Y.Y. and Li, Hsiang-Nan and Sanda, A.I. (2001), Phys.Rev. D63 054008, hep-ph/0004173.

[90] Wei, Zheng-Tao and Yang, Mao-Zhi (2002), Nucl.Phys. B642 263, hep-ph/0202018.

[91] Wirbel, M. and Stech, B. and Bauer, Manfred (1985), Z.Phys. C29 637.

[92] Zhang, Zhi-Qing and Xiao, Zhen-Jun (2009), Commun.Theor.Phys. 51 885.

[93] Ball, Patricia and Zwicky, Roman (2005), Phys.Rev. D71 014015, hep-ph/0406232.

[94] Mahajan, Namit (2004), hep-ph/0405161.

[95] Li, Hsiang-nan (2002), Phys.Rev. D66 094010, hep-ph/0102013.

[96] Kurimoto, T. and Li, Hsiang-nan and Sanda, A.I. (2002), Phys.Rev. D65 014007, hep-ph/0105003.

[97] Li, Hsiang-nan and Mishima, Satoshi (2009), Phys.Rev. D80 074024, arXiv: 0907.0166.

[98] Choi, Ho-Meoyng and Ji, Chueng-Ryong (2007), Phys.Rev. D75 034019, hep-ph/0701177.

[99] Yeh, Tsung-Wen (2002), Phys.Rev. D65 074016, hep-ph/0107192.

ABSTRACT

USING HEAVY FLAVORS TO STUDY NEW PHYSICS

by

KRISTOPHER J. HEALEY

August 2013

Advisor: Dr. Alexey A. Petrov

Major: Physics

Degree: Doctor of Philosophy

In this doctoral dissertation I discuss the possible standard model contributions to select leptonic heavy meson decay modes. Included are calculations of soft photon contributions to a di-lepton decay of B-mesons as well as two-particle hadronic unitary contributions to the rare di-leptonic decay of the neutral D meson. Additionally, constraints are calculated for two super-WIMP dark matter models from rare heavy flavor decays.

AUTOBIOGRAPHICAL STATEMENT

EDUCATION
2007 - 2013 : Ph.D. Physics, Wayne State University, MI, USA
Theoretical Particle Physics
2000 - 2005 : B.S. Applied Physics, Kettering University, MI, USA
Minor : Computational and Applied Mathematics
Concentration : Optics

PROFESSIONAL EXPERIENCE
2009 - 2013 : Graduate Research Assistant
Dept. of Physics and Astronomy, Wayne State University, MI, USA
2007 - 2009 : Graduate Teaching Assistant
Dept. of Physics and Astronomy, Wayne State University, MI, USA
2003 - 2005 : Materials and Process Modeling and Computation Co-Op
Sandia National Laboratory, Albuquerque, NM, USA

AWARDS AND HONORS
2011 : Thomas C. Rumble Fellowship, Wayne State University, MI, USA
2009 : Daniel R. Gustafson Graduate Student Teaching Award, Wayne State University, MI, USA
2005 : Outstanding Thesis Award, Kettering University, MI, USA

PROFESSIONAL TRAINING
2012 : Theoretical Advanced Study Institute (TASI), University of Colorado, Co, USA

ACADEMIC ACTIVITY
2012 : Invited Judge 1st Annual REU Mini-Symposium, Wayne State University, MI, USA
2004 : President of the Society of Physics Students, Kettering University, MI, USA

PUBLICATIONS
Faking $B_s \to \mu^+\mu^-$
Y. G. Aditya, K. J. Healey and A. A. Petrov, arXiv:1212.4166 [hep-ph].

Searching for super-WIMPs in leptonic heavy meson decays
Y. G. Aditya, K. J. Healey and A. A. Petrov, Phys. Lett. B **710**, 118 (2012)
[arXiv:1201.1007 [hep-ph]].

Coupled Computer Simulations of Recrystallization in Deformed Polycrystals
C.C. Battaile, K.J. Healey, E.A. Holm
Materials Science Forum, 467-470, 641 (2004)

A Subgrain Growth Model for Strain-Free Nucleation during Recrystallization
K.J. Healey, E.A. Holm, M.A. Miodownik
Materials Science Forum, 467-470, 611 (2004)